ACS Partner Journal

CHEM & BIO ENGINEERING

pubs.acs.org/ChemBioEng

Review

4D Printing of Shape-Morphing Liquid Crystal Elastomers

Published as part of Chem & Bio Engineering virtual special issue "3D/4D Printing".

Tongzhi Zang, Shuang Fu, Junpeng Cheng, Chun Zhang, Xili Lu,* Jianshe Hu,* Hesheng Xia,* and Yue Zhao*

Cite This: *Chem Bio Eng.* 2024, 1, 488−515

Read Online

ACCESS | Metrics & More | Article Recommendations

ABSTRACT: In nature, biological systems can sense environmental changes and alter their performance parameters in real time to adapt to environmental changes. Inspired by these, scientists have developed a range of novel shape-morphing materials. Shape-morphing materials are a kind of "intelligent" materials that exhibit responses to external stimuli in a predetermined way and then display a preset function. Liquid crystal elastomer (LCE) is a typical representative example of shape-morphing materials. The emergence of 4D printing technology can effectively simplify the preparation process of shape-morphing LCEs, by changing the printing material compositions and printing conditions, enabling precise control and macroscopic design of the shape-morphing modes. At the same time, the layer-by-layer stacking method can also endow the shape-morphing LCEs with complex, hierarchical orientation structures, which gives researchers a great degree of design freedom. 4D printing has greatly expanded the application scope of shape-morphing LCEs as soft intelligent materials. This review systematically reports the recent progress of 3D/4D printing of shape-morphing LCEs, discusses various 4D printing technologies, synthesis methods and actuation modes of 3D/4D printed LCEs, and summarizes the opportunities and challenges of 3D/4D printing technologies in preparing shape-morphing LCEs.

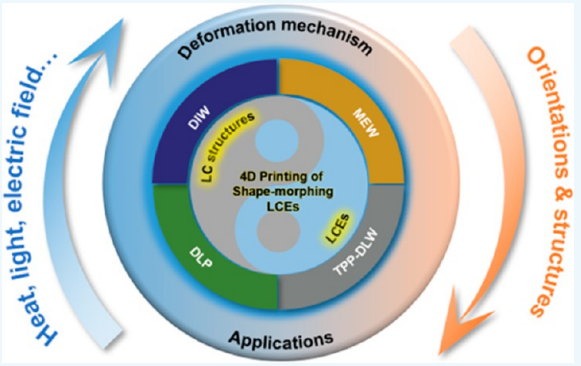

KEYWORDS: *3D printing, 4D printing, Shape-morphing materials, Liquid crystal elastomers, Actuators*

1. INTRODUCTION

Additive manufacturing, commonly referred to as 3D printing, stands as a revolutionary manufacturing technology that constructs objects layer by layer utilizing digital models and specialized materials.[1] Compared with the traditional subtractive manufacturing process, it has the superiorities of high efficiency, flexibility and environmental protection, and can achieve the goals of complex structures, personalized customization and functional integration. Additive manufacturing technology spans various disciplines, including machinery, materials, computer vision, software, electronics and so on. Its core is the manufacturing of 3D printers, and it also has special requirements for materials, software, design and so on. According to the definition provided by the American Society for Testing and Materials (ASTM), additive manufacturing technologies can be categorized into seven major groups: powder bed melting (PBF), directed energy deposition (DED), binder jetting (BJ), material extrusion (ME), light curing (VAT), laminate lamination (SLM), and bioprinting (BP).[1]

3D printing technology has become increasingly popular since the 1980s. The structures fabricated by 3D printing technology are usually static and stable, but lack changeable features. Therefore, 4D printing technology has emerged. In 2013, MIT scholar Skylar Tibbits first put forward the concept of 4D printing in a TED talk titled "The Emergence of 4D Printing".[2] 4D printing introduces the dimension of time on the basis of 3D printing, which can be simply described as "3D printing + time" or "3D printing + smart materials".[3] In the 4D printing process, people employ the principles of 3D printing but enhance the process by utilizing intelligent materials with various stimuli-responsive characteristics.[3] Based on the printed models digitally built by software, the initially 4D printed structure will undergo properties change over time according to the programming settings, under exposure to external stimuli (such as water,[4,5] light,[6] heat,[7] magnetic fields,[8] pH,[9] etc.). Compared with traditional 3D printing, the manufacturing concept of 4D printing has evolved from fixed structure to dynamic variable

Received: January 31, 2024
Revised: May 22, 2024
Accepted: May 22, 2024
Published: June 3, 2024

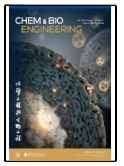

https://doi.org/10.1021/cbe.4c00027
Chem Bio Eng. 2024, 1, 488−515

structure design and manufacturing. The emergence of 4D printing not only makes it possible to construct macroscopic and complex 3D structures but also imparts unique intelligence to the printed structures. The 4D printed materials can respond to external stimuli and alter their structure or function. Therefore, 4D printing has promising application prospects in the fields such as biomedicine,[10,11] robotics,[12,13] military,[14] architecture,[15] and others. As illustrated in Figure 1, it is evident that the

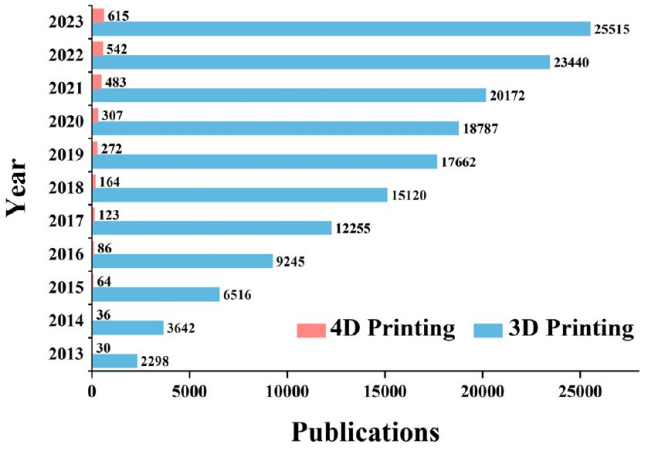

Figure 1. Trend chart showing the number of publications on 3D and 4D printing between 2013 and 2023 counted from Web of Science (Source: webofscience.com; the data were collected until April 2024).

quantity of research papers on the subject of 4D printing has consistently risen since the inception of the concept in 2013. However, in comparison to traditional 3D printing, 4D printing is still in its early stage of development. As Prof Qi emphasized, 4D printing will develop rapidly in the next decade after its inception.[16] Now is the time.

The increasing demand for 4D printing has significantly promoted the development of 4D printed materials. While conventional materials such as plastics are suitable for 3D printing, the majority of 3D printed materials are not well-suited for 4D printing because these materials cannot respond to external stimuli. 4D printed materials should possess two characteristics: printability and intelligence. If the materials cannot be printed with existing printing techniques, then the 4D printed structures will not be fabricated. For example, thermosetting resins cannot be applied to fused deposition modeling (FDM), which requires the materials to be melted. On the other hand, if the materials lack intelligence capacity and cannot change over time under external stimuli, they could not be regarded as 4D printed materials. Therefore, the most straightforward method to accomplish 4D printing is the 3D printing of a smart material. Smart material is a novel multifunctional material capable of sensing changes in the external environment and proactive responsiveness.[17] The fundamental approach of 4D printing involves precise control of local internal stress within the printed structure, and predictable triggering of shape changes upon subsequent release of the internal stress.

As a prominent representative of shape-morphing materials, LCE can undergo reversible, large and rapid shape changes under external stimuli because of both the anisotropy of liquid crystal and the soft elasticity of elastomer.[18] The LCEs exhibit a reversible phase transition in the mildly crosslinked liquid crystal polymer network, enabling a typical bidirectional shape memory effect. Upon heating, the liquid crystal mesogens oriented along a specific direction become isotropic, resulting in contraction of the bulk material. After cooling, the liquid crystal mesogens can return to their original ordered state and enable the recovery of the initial shape of the LCE, leading to a macroscopic reversible shape change. Compared with other stimuli-responsive polymers, the rapid and reversible shape change of LCEs and the versatility of reprogramming temporary shapes make LCEs ideal materials for fabricating soft smart devices.[19,20] To achieve deformations of LCEs, it is necessary to orient and fix the liquid crystal mesogens through crosslinking. Traditional preparation methods such as the "one-step method" and "two-step crosslinking method" are relatively complicated, and have some limitations on the selection of materials and structural design, so how to prepare LCEs with complex deformation modes by simple methods is still a challenge.[21] 4D printing of LCEs not only streamlines the preparation process of LCEs, but also endows them with complex deformation modes by programming.[22]

With the rapid development of 4D printed LCEs, several excellent reviews of 4D printed LCEs have emerged.[18,22−26] In this review paper, from the perspective of materials chemistry, we comprehensively introduce the structural characteristics of liquid crystal molecules, and the orientation methods of LCEs. Furthermore, we summarize and analyze the 4D printed LCE techniques, including the printing principles, ink composition, orientation, resolution, advantages, and disadvantages of various printing methods in detail. Additionally, we discuss the applications of 4D printed LCEs in the field of biomimetic soft robots, micro-mechanical devices & bionic actuators, optical applications, LCE lattice structures and dissipators. We summarize the printing techniques, printing structure, actuation mode and deformation mode of various 4D printing shape-morphing LCEs in detail. Finally, we discuss the challenges faced by 4D printing of shape-morphing LCEs and envision the possible future development trends. We have summarized the whole review topics of this review in Figure 2.

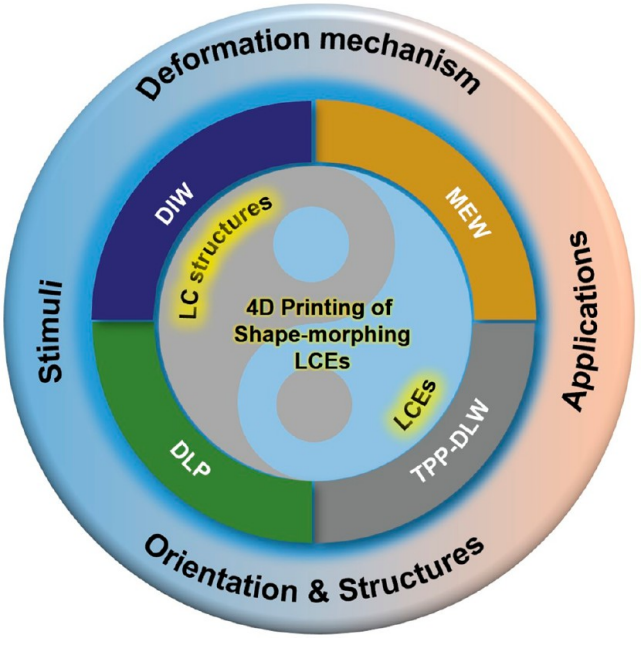

Figure 2. Overview of this review.

https://doi.org/10.1021/cbe.4c00027
Chem Bio Eng. 2024, 1, 488−515

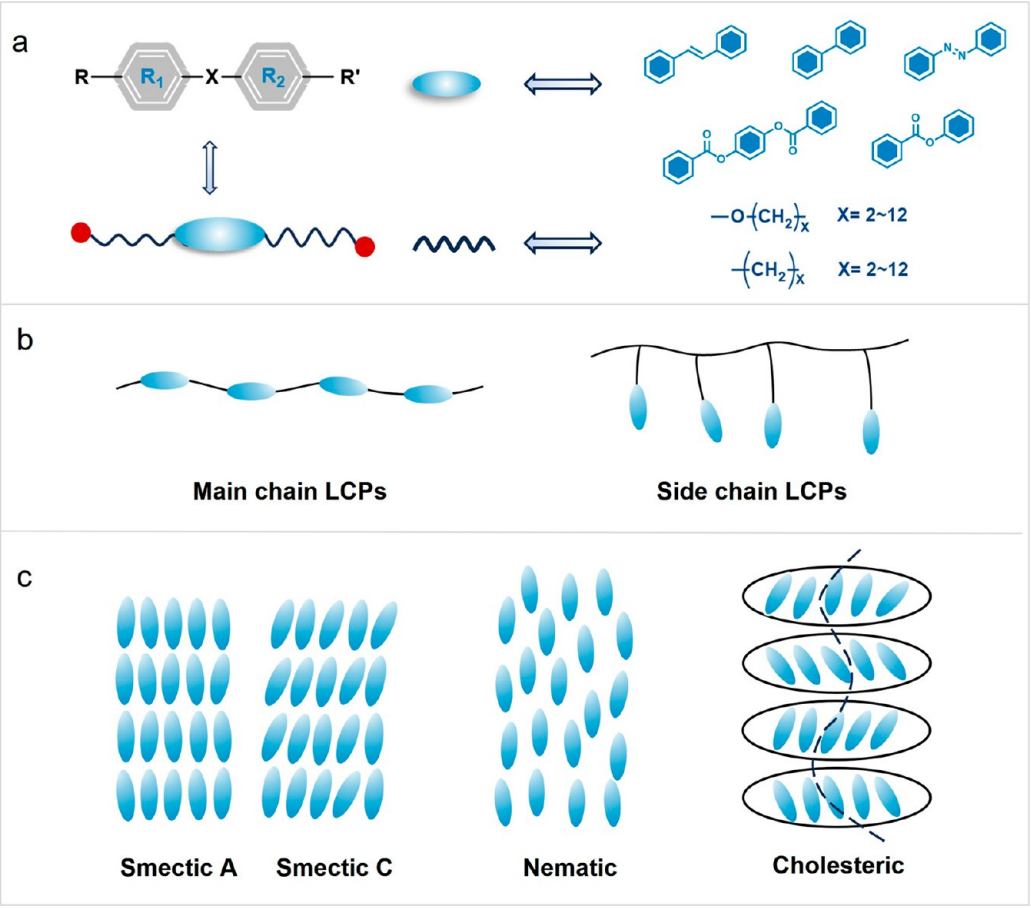

Figure 3. (a) Structure diagram of liquid crystal molecules. (b) Schematic illustrations of the formation of main chain LCPs and side chain LCPs. (c) Structure diagram of common liquid crystal phases.

2. LIQUID CRYSTALS

Liquid crystals were discovered in the late 19th century by Reinitzer, an Austrian plant scientist, when he used a microscope to observe the melting of the compound cholesteryl benzoate. More than 100 years after the discovery, people have not stopped the studies of liquid crystals. O. Wiener et al. developed the birefringence theory of liquid crystals; E. Bose proposed the phase state theory of liquid crystals; V. G. Jean et al. studied the molecular orientation mechanism and texture of liquid crystals; and so on. It is worth mentioning that de Gennes was awarded the Nobel Prize in Physics in 1991 for recognition of his exceptional contributions to the field of liquid crystal research. In nature, condensed matter can be classified into liquid state, crystalline state, liquid crystal state and plasma state according to the different order degree of its microstructure. Among these, liquid crystal state is a kind of special form of matter between liquid state and crystalline state, it possesses the fluidity and continuity characteristic of an isotropic liquid state while concurrently exhibiting the typical anisotropy of a crystalline state.[19] Liquid crystals can make reversible transitions between ordered and disordered states. In the ordered state, the liquid crystal molecules are arranged in a well-defined manner, resulting in anisotropy. In the disordered state, the liquid crystal units are randomly distributed and become isotropic, and the temperature at which this transition occurs is referred to as the liquid crystal order-disorder phase transition temperature ($T_{LC\text{-}Iso}$). The liquid crystal materials can be small molecules or macromolecules, but their liquid crystal units are generally composed of rigid, rod-like or long strip molecules (Figure 3a). The core units R_1 and R_2 are usually aromatic or aliphatic rings connected by bridging bonds -X- (−COO-, -N═N(O)-, etc.), which can provide the required anisotropy of liquid crystal molecules. Nonetheless, only a rigid framework is not sufficient to induce the liquid crystal phase, and it is necessary to attach the flexible chain segments or the polarizable groups R or R′ at its ends, which is usually composed of branched alkyl or alkoxy and other structures, thus a low melting point liquid crystal molecule can be obtained and the molecular arrangement of the mesophase structure is stable.

Based on the molecular weight, liquid crystals can be categorized as small molecule liquid crystals, oligomers, low molecular weight polymers, liquid crystal polymers. In terms of their origin, liquid crystals can be categorized into natural polymer liquid crystals (such as celluloses, polypeptides, proteins, nucleic acid macromolecules) and synthetic polymer liquid crystals (including polyamide, polyaryl ester, poly(methyl methacrylate), and silicone). Depending on the conditions of their formation, liquid crystals can be classified into two main categories: thermotropic liquid crystals and lyotropic liquid crystals. Specifically, thermotropic liquid crystal is heated to the liquid crystal state, while lyotropic liquid crystal state is achieved by adding solvent. According to the features of the chain structure, liquid crystal polymers can be classified into main chain LCPs (with the liquid crystal cores incorporated in the main polymer chain) and side chain LCPs (featuring liquid crystal cores attached to the side chain) (Figure 3b).

https://doi.org/10.1021/cbe.4c00027
Chem Bio Eng. 2024, 1, 488−515

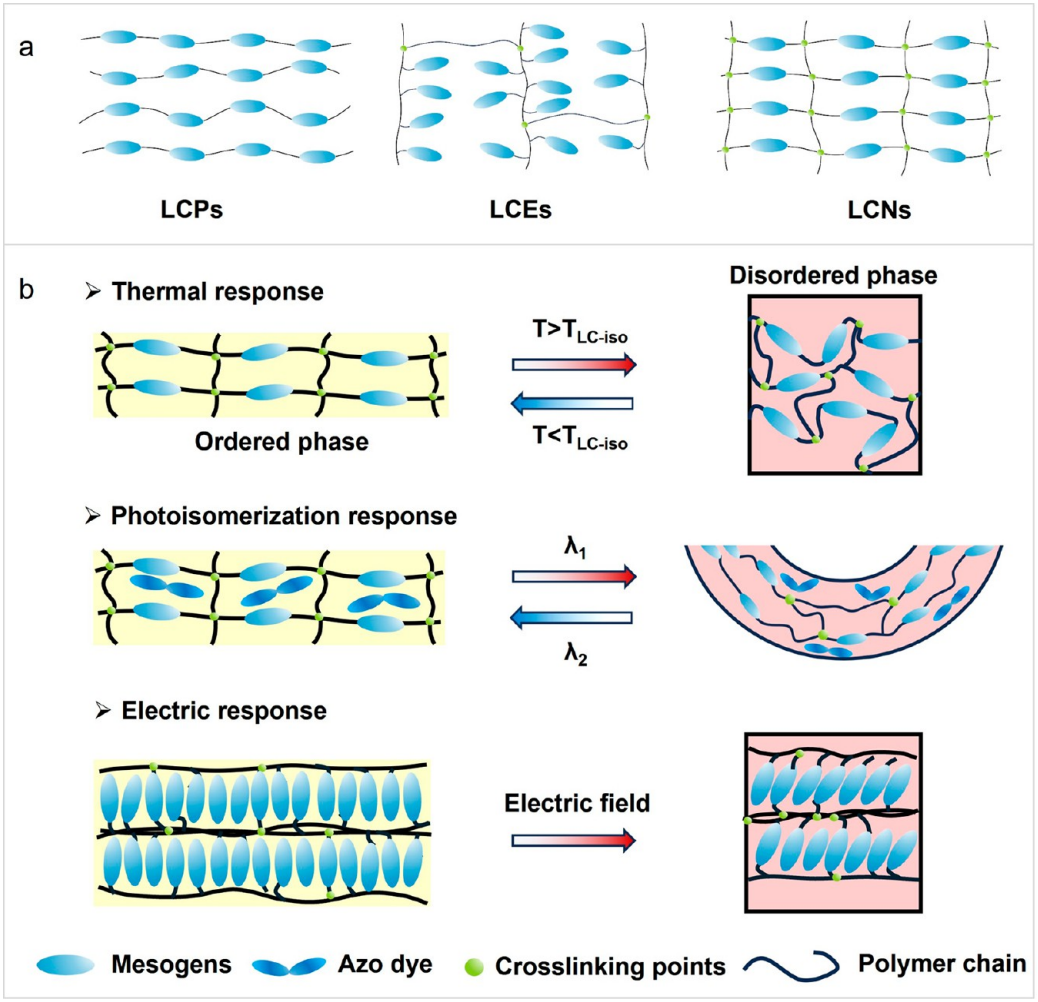

Figure 4. (a) Structure diagram of LCPs, LCEs, and LCNs. (b) Structure diagram of the mechanism of reversible deformation of LCE actuators.

Additionally, liquid crystals can be further categorized based on their phase characteristics into nematic liquid crystals, cholesteric liquid crystals and smectic liquid crystals (Figure 3c).

The nematic phase is the most prevalent liquid crystal phase, characterized by a relatively low degree of order, specifically one-dimensional orientational order. In this phase, molecules do not form layers but align themselves in parallel, with their long axes roughly pointing in the same direction. The molecular arrangement in the nematic phase is characterized by its irregularity, allowing for sliding movements in various directions, back and forth, left and right, up and down. Consequently, this phase exhibits low viscosity and significant fluidity. The smectic phases exhibit higher degrees in ordered molecular arrangements, displaying a two-dimensional order. The molecules are organized in a layered structure parallel to each other, and the long axes of the molecules in the layer are parallel to each other, arranged neatly, and perpendicular to the layer (smectic A phase) or form a certain angle (smectic C phase). Under certain conditions, the smectic A and smectic C phases can undergo a reversible phase transition.[27] While these molecules maintain lateral mobility within the layer and exhibit fluidity, their viscosity remains significantly high. Nonetheless, these molecules are unable to traverse between the layers, leading to a high degree of order, which is typically observed at lower temperatures. The cholesteric phase can be regarded as a special nematic liquid crystal. In cholesteric phase, molecules are organized into layers, with each layer exhibiting parallel alignment of its constituent molecules. However, the long-axis orientation of the molecules between layers is systematically twisted at a certain angle. These twisted layers stack on top of each other, resulting in a spiral structure, and this arrangement imparts its unique optical properties and behaviors.

3. LIQUID CRYSTAL ELASTOMERS

Since Finkelmann first reported the preparation of LCEs by secondary crosslinking method in 1981, research in the field of LCEs has entered a new era.[28] Liquid crystal polymers (LCPs) are obtained by connecting small liquid crystal molecules through covalent bonds. Liquid crystal networks (LCNs) can be obtained by high cross-linking LCPs. In contrast, LCEs are obtained by slight cross-linking of LCPs (Figure 4a). LCEs are a class of special elastomers that exhibit elasticity in both isotropic and liquid crystal states. Because they combine the rubbery elasticity of polymer network and the anisotropy of liquid crystal, they have[29] good external responsiveness, molecular coordination, and elasticity.[29,30] They can produce a large macroscopic shape change by changing the arrangement of the liquid crystal elements under external stimuli. This reversible bidirectional memory of the stimuli-responsive shape changes makes LCEs have good stability,[31] rapid response,[32] large deformation,[33] good mechanical properties,[19] and other characteristics, and enables their wide use in the field of smart

https://doi.org/10.1021/cbe.4c00027
Chem Bio Eng. 2024, 1, 488−515

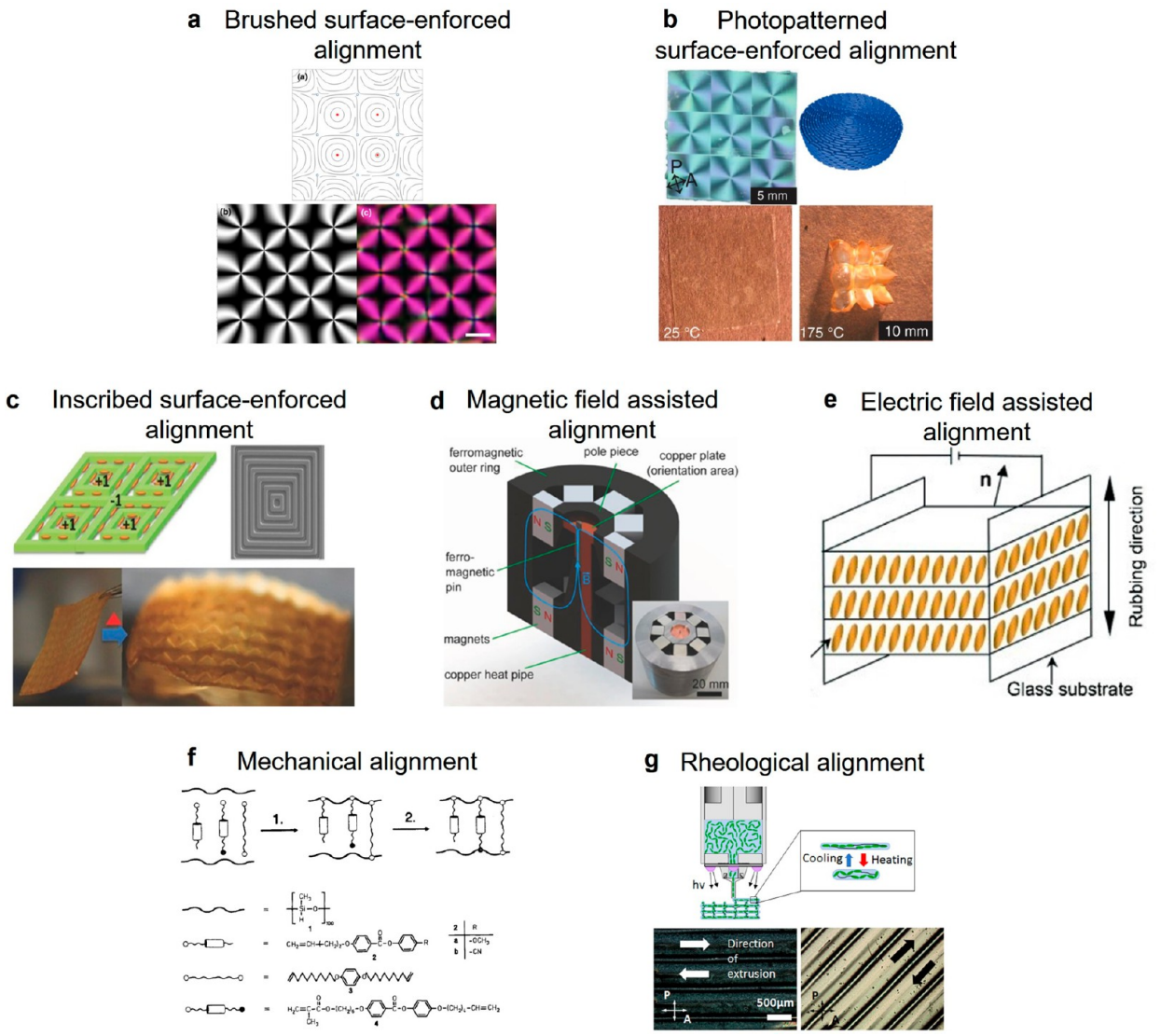

Figure 5. Orientation methods of LC mesogens. (a) Brushed surface-enforced alignment.[83] Reproduced with permission. Copyright 2014, American Physical Society. (b) Photopatterned surface-enforced alignment.[52] Reproduced with permission. Copyright 2015, American Association for the Advancement of Science. (c) Inscribed surface-enforced alignment.[51] Reproduced with permission. Copyright 2016, John Wiley & Sons, Inc. (d) Magnetic field assisted alignment.[43] Reproduced with permission. Copyright 2014, John Wiley & Sons, Inc. (e) Electric field assisted alignment.[90] Reproduced with permission. Copyright 2007, John Wiley & Sons, Inc. (f) Mechanical alignment.[91] Reproduced with permission. Copyright 1991, John Wiley & Sons, Inc. (g) Rheological alignment.[94] Reproduced with permission. Copyright 2017, American Chemical Society.

materials such as soft robotics & actuators,[31,34−40] artificial heliotropic devices,[41] rotating micro engines,[42] bionic implantable devices,[29,43−48] microfluidic devices[49] and so on.

3.1. Deformation Mechanism of LCEs. Firstly, LCEs that are cross-linked but lack a specific orientation are referred to as multi-domain or polydomain LCEs. In these elastomers, the liquid crystal elements lack a macroscopic and uniform arrangement and orientation, leading to random and limited deformations. As a result, the whole sample cannot effectively manifest a macroscopic change in shape. By orienting the liquid crystal mesogens in a specific direction, a monodomain LCE is obtained.[50] During the transition from the liquid crystal phase to the isotropic phase, the mesogens switch between order state and disorder state, resulting in a consistent change in their orientation. This phenomenon can be observed macroscopically throughout the entire sample.

Since LCEs are generally formed by thermotropic liquid crystals, thermally responsive deformation usually occurs.[51−56] Under external thermal stimulation, when the temperature of the LCE actuator rises above its phase transition temperature, the molecular chain orientation disappears, the degree of order decreases significantly, and the liquid crystal mesogens change from anisotropic to isotropic state, resulting in the material shrinking along the orientation direction. Upon cooling, the material undergoes an opposite process, extending along the orientation direction and returning to its original form (Figure 4b). LCEs functioned with photothermal dyes,[57−63] magnetic thermal fillers[64−66] and electric thermal fillers[38,67−69] are also essentially thermoresponsive LCEs. For intrinsic photosensitive LCEs, the *cis-trans* isomerization of photosensitive dyes affects the orientation of the LC mesogens, ultimately resulting in the macroscopic deformation of the LCEs[36,37,70−72] (Figure 4b). In addition, the external electric field can induce the rearrangement of LC mesogens, which subsequently facilitates the macroscopic contraction of LCEs[73−76] (Figure 4b). Further studies have

https://doi.org/10.1021/cbe.4c00027
Chem Bio Eng. 2024, 1, 488−515

found that LCEs can also be stimulated by chemical solvents,[77] and humidity[78−80] and make corresponding deformation.

3.2. Orientation of LCEs. The orientation of the LC mesogens and the formation of cross-linked anisotropic structures are critical factors for the preparation of LCEs with reversible deformation. In general, the preparation of LCE actuators can be categorized into two main approaches: the two-step cross-linking method and the one-step cross-linking method.[81] For the former, the pre-crosslinked LC gel is initially oriented through mechanical stretching or 3D printing, and the orientation is then retained by additional cross-linking to stabilize the aligned structure. For the latter, LCE is formed by direct polymerization of low molecular weight liquid crystal monomers after ordered alignment. While each orientation method possesses distinct characteristics, several common challenges must be addressed. The first is that during the process of orientation, the material needs to be in the liquid crystal phase. Additionally, the cross-linking reaction must be conducted under conditions that preserve the alignment of the LC elements.

3.2.1. One-Step Cross-Linking Method. The one-step cross-linking method is to directly obtain a monodomain LCE by initiating the cross-linking reaction of the ordered liquid crystal elements. In this method, polymerizable LC elements, multifunctional crosslinker, and photoinitiator are blended in specific proportions and directly added to the liquid crystal cell, or subjected to magnetic field or electric field. The polymerization reaction is then triggered through either ultraviolet irradiation or heat, resulting in the formation of LCEs.

(1) Brushed surface-enforced alignment. Brushed surface-enforced alignment is a standard technique in the liquid crystal display (LCD) industry to control large surface area alignment,[82] and friction creates microgrooves in glass substrates coated with planar anchored polyimide (PI)[83] or poly(vinyl alcohol) (PVA) (Figure 5a). Using this orientation method can prepare thin monodomain LCE films whose thickness is less than 100 μm.[84,85] However, it is difficult to control the resolution of liquid crystal orientation within a micron scale by friction.

(2) Photopatterned surface-enforced alignment. Ware et al. reported direct photopatterned surface-enforced alignment of multi-domain LCEs.[52] Based on the optical graphization method, they successfully prepared programmable topological shape changes for a variety of complex directional profiles (Figure 5b). The optical alignment technology allows alignment control within the optical resolution, and the LCE film thickness cannot exceed 50 nm. White et al. also use this technology to successfully prepare LCEs with topological structure.[53]

(3) Inscribed surface-enforced alignment. In 2012, Yu et al. prepared oriented LCEs by using highly oriented carbon nanotubes to induce the arrangement of LC mesogens.[86] They initially constructed a carbon nanotube sheet with a specific structural arrangement. Then, they introduced small liquid crystal molecules into this microarray, aligning the small liquid crystal monomers along the array structure. They subsequently triggered polymerization and cross-linking through ultraviolet light illumination, leading to the immediate formation of a monodomain LCE. In 2016, Yang et al. also successfully prepared oriented LCEs by using PDMS with a special groove structure as a template[51] (Figure 5c). In particular, grooves were first fabricated by stereolithography with high resolution. Later, liquid crystal molecules can easily be orientated in the groove. It is worth mentioning that the resolution of LCEs fabricated in this way can reach the level of several microns.

(4) Magnetic\electric field assisted alignment. Based on the anisotropic permittivity and diamagnetization of the liquid crystal elements, external stimuli such as electric and magnetic fields are suitable for aligning the liquid crystal arrangement. The polarity of the LCE monomer can be changed by introducing polar groups such as nitrile or ester which exhibit positive dielectric anisotropy.[87−89] Zappe et al. successfully designed a liquid crystal actuator by using an optimized, custom-designed radially oriented 100 mT magnetic field.[43] This liquid crystal actuator is electrically actuated to produce highly miniaturized, fully integrated apertures whose behavior can mimic the movement of the human pupil (Figure 5d). Inspired by the electric field alignment of LCEs, Yu et al. fabricated azobenzene LCE films under an electric field[90] (Figure 5e). LCEs prepared in this technology exhibit a relatively high degree of orientation. The film can be reversibly actuated under 366 nm UV and visible light irradiations.

Different from the two-step cross-linking method, the one-step cross-linking approach directly polymerizes low molecular weight liquid crystal monomers to prepare the LCE networks, omitting the pre-cross-linking, resulting in improved preservation of the oriented structure. Nevertheless, the oriented structure is typically obtained through surface induction, and the degree of orientation tends to decrease as the thickness increases. Therefore, the LCEs prepared by one-step method are usually thin films and require the use of low-viscosity liquid crystal monomers (reactive mesogens). Although the one-step method is simple and easy, with a high success rate, it can flexibly realize parallel or vertical orientation, and has a good control of crosslinking degree by changing the content of the cross-linking agent. However, there are some small molecules such as liquid crystal elements and cross-linking agents remain due to incomplete reactions in the LC cell, which affect the performance of the materials. Due to the limitations of surface alignment, most of the LCEs are small thin films, which have limitations in the design of the LCEs actuator.

3.2.2. Two-Step Cross-Linking Method. Finkelmann et al. developed the two-step cross-linking method to fabricate monodomain LCEs in 1991.[91] The two-step method refers to the synthesis of some liquid crystal prepolymers with special functional groups, whose orientation of the liquid crystal components is achieved through mechanical stretching or 3D printing, enabling subsequent cross-linking to obtain highly oriented mono-domain LCEs.

(1) Mechanical alignment. A straightforward two-step cross-linking approach is based on organosilicon chemistry.[91] Silyl hydrogen addition reaction is frequently used in the synthesis of side-chain LCEs.[92] Linear polysiloxane chains are blended with monovinyl functionalized LC monomers and multifunctional vinyl crosslinkers. Since the vinyl group reacts faster than the methacryloyl group, the cross-linking process can be carried out in two steps. The first reaction step generates low crosslinked polymers, with the molecular chains being aligned through mechanical stretching. Under the condition of maintaining the stress, the second stage polymerization reaction generates a

https://doi.org/10.1021/cbe.4c00027
Chem Bio Eng. 2024, 1, 488−515

strongly crosslinked polymer network and permanently fixes the orientation structure. This relatively straightforward method can be used to prepare highly oriented LCEs (Figure 5f). This method also can be extended to other systems with different liquid crystal monomers and crosslinkers. However, a potential issue with this method is the presence of low molar mass materials resulting from incomplete reactions, which could affect the material's performance. Main-chain LCEs can be prepared by a two-step acrylate Michael addition reaction and photopolymerization (TAMAP) reaction. Yakacki et al. first prepared a multidomain LC prepolymer by a sulfhydryl-acrylate "click" reaction.[93] After aligning the multidomain LC prepolymer by stretching, excess acrylate groups can undergo further cross-linking by photopolymerization.

(2) Rheological alignment. Ware and colleagues have fabricated oriented LCEs through DIW printing.[94] Specifically, during the DIW printing process, the orientation of LC mesogens is induced by the rheological field (Figure 5g). The DIW printing method allows the fabrication of LCEs along any desired path, an unparalleled capability compared to other methods. This approach imposes a high viscosity requirement on the ink, which should be effectively extruded through the nozzle before being cured.[95]

The two-step method has been widely used by researchers since its development; however, the procedure is relatively tedious, and the inherent conflict between the degree of orientation and the degree of cross-linking imposes a significant limitation on this reaction. To obtain better actuation performance, it is essential to achieve higher orientation. Although good orientation can be achieved under high elongation, if the crosslinking degree of the first step is reduced, the gel's strength becomes weaker and more susceptible to tensile fracture. However, if the crosslinking degree of the first step is increased, the movement of the liquid crystal elements is restricted and a higher orientation cannot be obtained.

LCEs with dynamic bonds offer a solution to address the above problems.[96] Inspired by the properties of Vitrimer, Pei et al. proposed a method to fabricate monodomain LCE vitrimer in 2013.[97] They initially prepared LCEs containing dynamic cross-linked ester bonds. Subsequently, dynamic ester bonds are activated at high temperatures to orient the liquid crystal mesogens by mechanical stretching. The rapid transesterification reaction induces a reconfiguration of the crosslinked LCE network. This LCE network can fix the orientation upon cooling, resulting in a monodomain LCE. Furthermore, they introduced carbon nanotubes (CNTs) into this system to prepare LCE/CNTs composites containing dynamic cross-linked ester bonds.[61] By utilizing the photothermal effect of CNTs to activate dynamic ester bonds at high temperatures, the actuator is endowed with photoactivated remodeling properties to meet various complex environmental requirements. Up to now, dynamic bonds such as transesterification, Diels-Alder bonds, disulfide bonds, and metal coordination bonds have been incorporated into LCEs, and the rapid development of dynamic LCEs has largely broadened the applications of deformable LCEs.[98]

To sum up, the orientation methods of liquid crystal elements mainly include brushed surface-enforced alignment, photopatterned surface-enforced alignment, inscribed surface-enforced alignment, magnetic field-assisted alignment, electric field-assisted alignment, mechanical alignment and rheological alignment. For different applications, it is essential to judiciously select the suitable orientation method of LC mesogens based on the chemical structures of the LC monomers and the dimensions of the LCE actuators. Here, the characterization of different alignment methods of LCEs is summarized in Table 1.

Table 1. Summary of Strategies for Orientation of Liquid Crystal Elastomers

Orientation method of liquid crystal elastomers	Advantages and disadvantages
Brushed surface-enforced alignment	· Simple process · The resolution does not reach the micrometer-scale
Photopatterned surface-enforced alignment	· Micrometer resolution · High ink viscosity requirements
Inscribed surface-enforced alignment	· Micrometer resolution · The film thickness is less than 100 μm
Magnetic field-assisted alignment	· Suitable for preparing microcolumn array structure · Difficult to manufacture on a large scale
Electric field-assisted alignment	· Suitable for polar liquid crystal mesogens · Difficult to manufacture on a large scale
Mechanical alignment	· Simple process and can fabricate large-scale LCEs · Difficult to fabricate LCEs with different molecular orientations
Rheological alignment	· Print along any path with the utmost degree of freedom · The ink should be effectively extruded through the nozzle before being cured

4. 4D PRINTING OF LIQUID CRYSTAL ELASTOMERS

As mentioned above, there are certain limitations in the fabrication of LCEs using the traditional "one-step" or "two-step" method. On the one hand, it is necessary to prepare liquid crystal cells or introduce electromagnetic fields to induce the orientation of LC mesogens. On the other hand, the obtained monodomain LCEs are mostly sheet or membrane, which restricts the structure of the actuator. The emergence of 4D printing technology can not only simplify the preparation process of the LCEs, but also afford the actuators with complex structures and unique orientation modes. The fabrication of LCE actuators through 4D printing technology offers advantages such as precise control of the orientation structure of LC elements and the convenient design of macroscopic shapes. This not only simplifies the preparation process of traditional LCE actuators but also allows for the creation of complex, multi-level orientation structures through layer-by-layer stacking, which provides the researchers with great design freedom. 4D printing has become a research hotspot in the field of LCEs.[22,24,99,100] However, the higher controllable degrees of 4D printing also present increased demands on the orientation of LC mesogens. The most important 4D printing method for LCE is DIW, MEW has advantages in the fabrication of ultra-fine LCE fibers, while 2PP-DLW and DLP have gradually attracted researchers' interest because of their submicron control ability. Figure 6 illustrates the schematic diagram of the principles for the above four printing methods.

4.1. Printing Method. *4.1.1. DIW.* DIW is the most commonly employed technology for LCE printing owing to its wide material compatibility and printing flexibility.[35,94,95,101−104] The inks used in DIW are usually liquid

https://doi.org/10.1021/cbe.4c00027
Chem Bio Eng. 2024, 1, 488−515

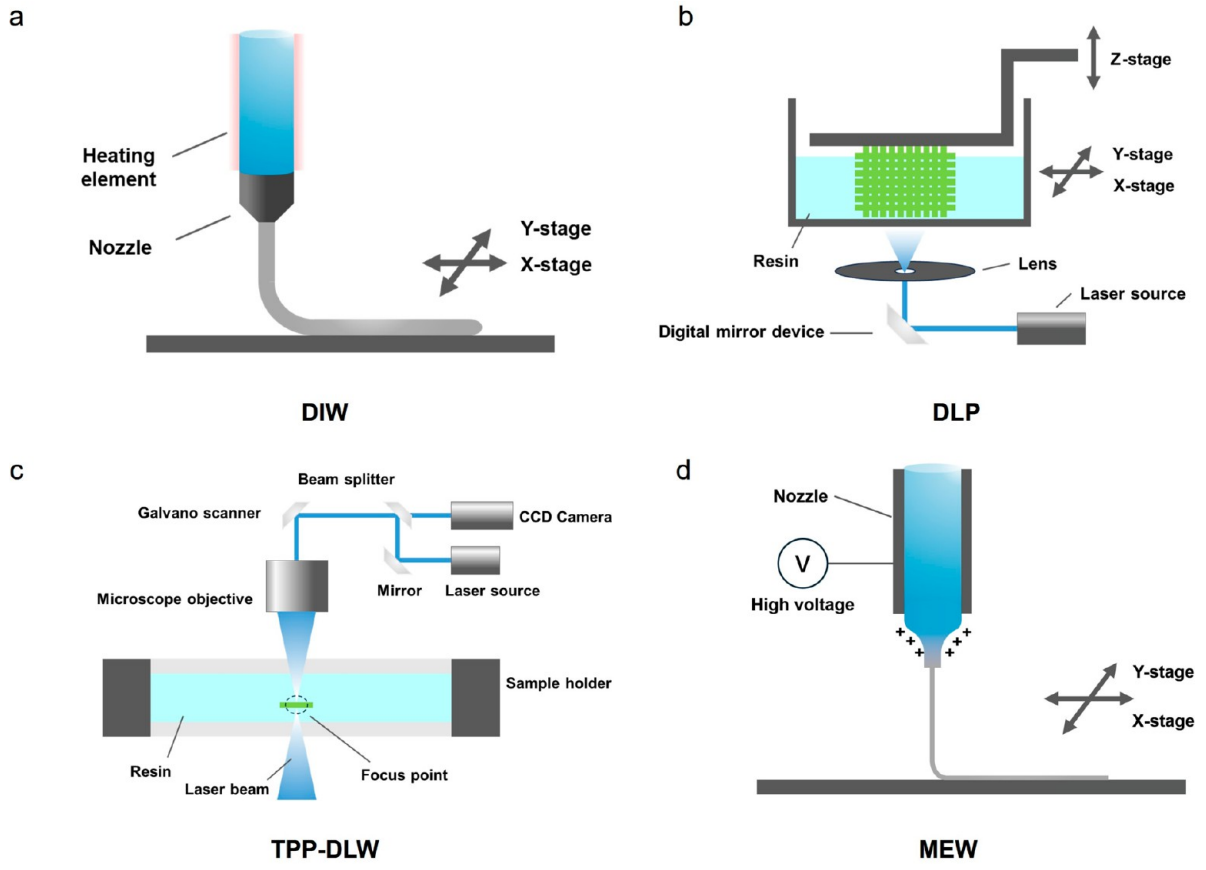

Figure 6. Schematic diagram of the printing methods of LCEs. (a) DIW, (b) DLP, (c) TPP-DLW, and (d) MEW.

crystal oligomers with typical shear-thinning characteristics. These oligomers are produced by the addition reaction of LC monomers with chain extenders or single-component LC oligomers. Shear-thinning property facilitates the extrusion of viscous ink from the nozzle under the influence of airflow or screw pressure. In the extrusion process, the ink undergoes shear force to form anisotropic filaments, which are subsequently deposited on the printing platform, aligning liquid crystal elements in a predetermined printing path. Therefore, the spatial arrangement of liquid crystal orientation can be designed by adjusting the movement trajectory of the nozzle. Filaments extruded through shear force can temporarily maintain their shape and ordered structure and be fixed in the subsequent step through photo-cross-linking. Ware et al. first used the HOT-DIW technique to fabricate the first 3D structured LCE actuators with aligned molecular orientation in 2017[94] (Figure 7a). They prepared DIW-printable inks, which were subsequently extruded and ordered along the printing path and then cross-linked by UV irradiation. The oriented filament could undergo 40% reversible contraction and extension upon heating and cooling, respectively. They printed LCE structures with regions of opposite Gaussian curvature that can reversibly and rapidly deform upon heating and cooling. For DIW printing, the actuation performance of LCE is highly related to the printing materials and printing parameters. Wang et al. prepared DIW-printable inks and systematically investigated the influence of printing temperature, nozzle size, and the nozzle-to-substrate distance on the actuation characteristics.[102] The results showed that higher printing temperature, larger nozzle diameter, and larger gap lead to smaller actuation strain. Higher printing temperatures and larger gaps also resulted in reduced actuation stress. Furthermore, their research revealed that the printing speed had no significant impact on the actuated strain.

In the previously mentioned example, cross-linking was achieved by self-polymerization of excess acrylate under UV irradiation after the completion of printing. Apart from the conventional photo-cross-linking method, two-stage amine-acrylate Michael addition reaction[105] have been used to maintain the printed shape and oriented structure. Zou et al. used a combination of RM82 and 1,5-diaminopentane to prepare inks for 4D printing of LCEs. In the first reaction stage, primary amines are completely consumed and acrylates are still in excess, crosslinking is achieved by Michael addition between secondary amines and acrylate-ended oligomers[105] (Figure 7b). It should be noted that the viscosity of the ink and the optimum printing time can be adjusted by adjusting the amount of diamine and solvent. In general, it is easier to obtain highly oriented LCEs with a lower amount of solvent. In addition, by eliminating the need for light to initiate the second stage of the cross-linking reaction, this strategy has great advantages in the preparation of azobenzene-containing LCEs, since azobenzene molecules usually have strong absorption of light that affects the second stage of photo-crosslinking reaction.

The flexibility of DIW printing technology allows for more design space to achieve adjustable performances and multiple functions of LCEs through the improvement and upgrading of printing equipment and the integration of multifunctional materials. The improvement of DIW printing equipment mainly focuses on the processing of nozzles and extruded filaments. These improvements include the utilization of nozzles with core-shell structures[103] and the implementation of rotatable substrates,[106,107] which enable the preparation of three-dimen-

https://doi.org/10.1021/cbe.4c00027
Chem Bio Eng. 2024, 1, 488−515

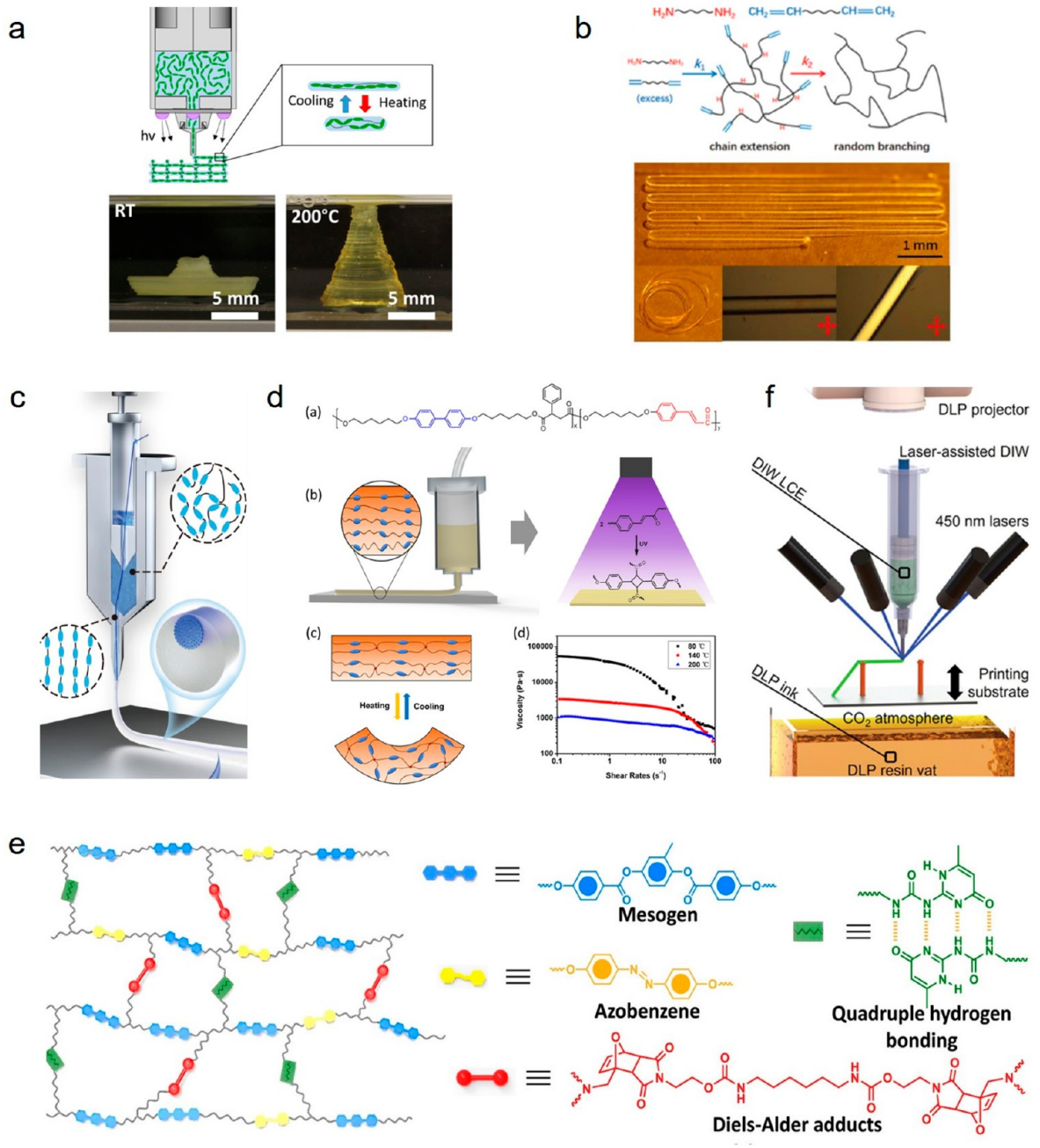

Figure 7. LCEs fabricated by DIW printing. (a) DIW-printed LCE structures with regions of opposite Gaussian curvature can reversibly and rapidly deform upon heating and cooling.[94] Reproduced with permission. Copyright 2017, American Chemical Society. (b) Two-stage Michael addition reaction to prepare LCEs.[105] Reproduced with permission. Copyright 2021, John Wiley & Sons, Inc. (c) DIW printing strategy for continuous fiber-reinforced LCE composites.[112] Reproduced with permission. Copyright 2023, Springer Nature. (d) High-temperature DIW printing of LCE inks with high viscosity.[56] Reproduced with permission. Copyright 2019, American Chemical Society. (e) DIW printed LCEs capable of maintaining long-term retention of a deformed state.[71] Reproduced with permission. Copyright 2020, John Wiley & Sons, Inc. (f) The combination of active LCE materials and inactive support materials to realize DIW 3D printing.[108] Reproduced with permission. Copyright 2022, John Wiley & Sons, Inc.

sional LCE tubes or long fibers. In addition, the combination of DIW and DLP[108] through hybrid additive manufacturing has recently been reported. An effective strategy to improve the mechanical properties of LCEs and to endow them with multiple stimuli responsiveness, such as optical, magnetic or electrical functions, is to introduce functional fillers into LCEs, such as carbon nanotubes,[109] gold nanorods[110] and titanium-based nanocrystals,[111] which endow LCEs with photothermal actuation and photochromism properties. The incorporation of liquid metals facilitates joule heating and self-induction properties of LCEs, whereas the incorporation of magnetic particles enables the LCEs to be magnetically and thermally actuated. However, it is also difficult to develop composite inks, because DIW has certain requirements for the rheological properties of the ink, and nano-fillers tend to aggregate owing to their extensive specific surface area. Therefore, it is an effective solution to print LCE ink and functional filler independently, such as using a nozzle with a core-shell structure to isolate the extrusion of LCE ink and LM ink, rather than preparing a mixed LM/LCE ink. Recently, Wang et al. have developed a DIW

https://doi.org/10.1021/cbe.4c00027
Chem Bio Eng. 2024, 1, 488−515

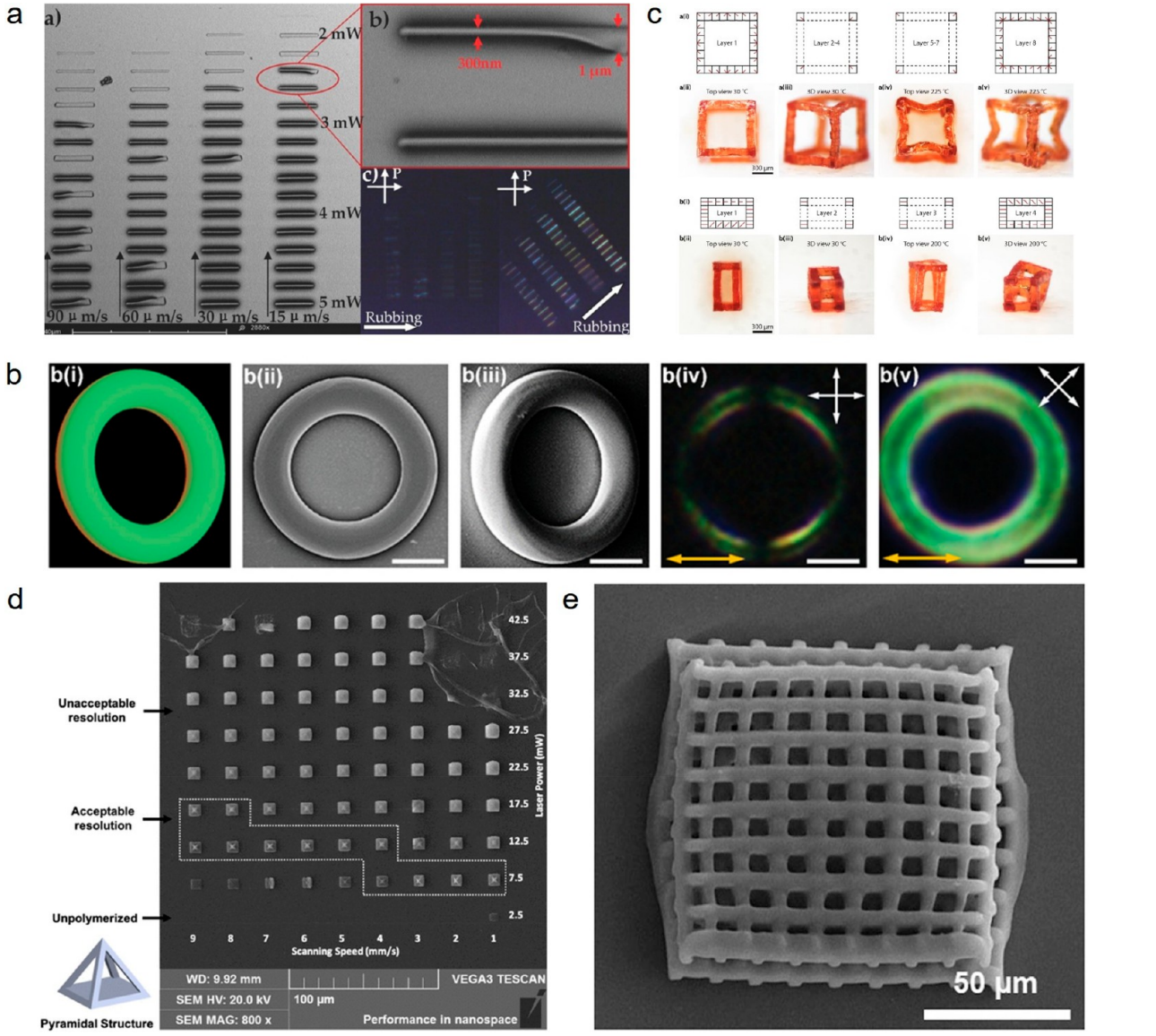

Figure 8. LCEs fabricated by TPP-DLW printing. (a) LCE structures with submicron resolution fabricated by TPP-DLW printing.[115] Reproduced with permission. Copyright 2014, John Wiley & Sons, Inc. (b) Spiral coil structure fabricated by TPP-DLW.[77] Reproduced with permission. Copyright 2020, John Wiley & Sons, Inc. (c) LCE cubes fabricated by TPP-DLW enabling complex shape transformations.[116] Reproduced with permission. Copyright 2021, Springer Nature. (d) SEM images of AuNR/LCEs composite materials fabricated by TPP-DLW.[117] Reproduced with permission. Copyright 2019, American Chemical Society. (e) SEM images of CNT/LCEs composite materials fabricated using TPP-DLW.[118] Reproduced with permission. Copyright 2020, Walter de Gruyter.

strategy for continuous fiber-reinforced LCE composites, where continuous fibers are extruded by a chamber structure with eccentric channels and coated with LCE ink[112] (Figure 7c). The incorporation of continuous fibers not only improves the mechanical properties of LCE, but also serves as a support structure during the printing process, enabling the direct 3D printing of structures. By selecting the eccentric position of the continuous fibers in the extruded filament, the direction of bending deformation in the composite can be controlled.

For DIW extrusion technology to prepare LCEs, in addition to the need for the ink to possess shear thinning characteristics, suitable ink viscosity is also required. The ink needs to be able to pass through the nozzle at a low temperature to form an oriented structure that can temporarily maintain its shape and orientation after extrusion. The orientation can be regulated by adjusting the printing parameters and printing path. Smaller nozzle diameter and higher printing speed generally result in better molecular alignment, but this also places higher demands on the rheological properties of the LCE ink. To overcome the challenges mentioned above, our group has introduced a novel strategy to achieve 4D printing at temperatures exceeding the T_{NI} of LCE.[56] Different from the commonly employed Michael addition strategy, we utilized biphenyl liquid crystal as the printing monomer. Initially, we synthesized a biphenyl liquid crystal prepolymer through molecular structure design, which incorporated phenyl side groups and cinnamic acid groups. The rheological experiment shows that the ink viscosity decreases at 200 °C, which can be extruded smoothly. The extruded liquid crystal ink could effectively maintain its printed shape because of the supramolecular interaction ($\pi-\pi$ stacking) of the phenyl side groups. Finally, the cross-linking was completed by the photo-crosslinking reaction of cinnamic acid groups, and the

https://doi.org/10.1021/cbe.4c00027
Chem Bio Eng. 2024, 1, 488−515

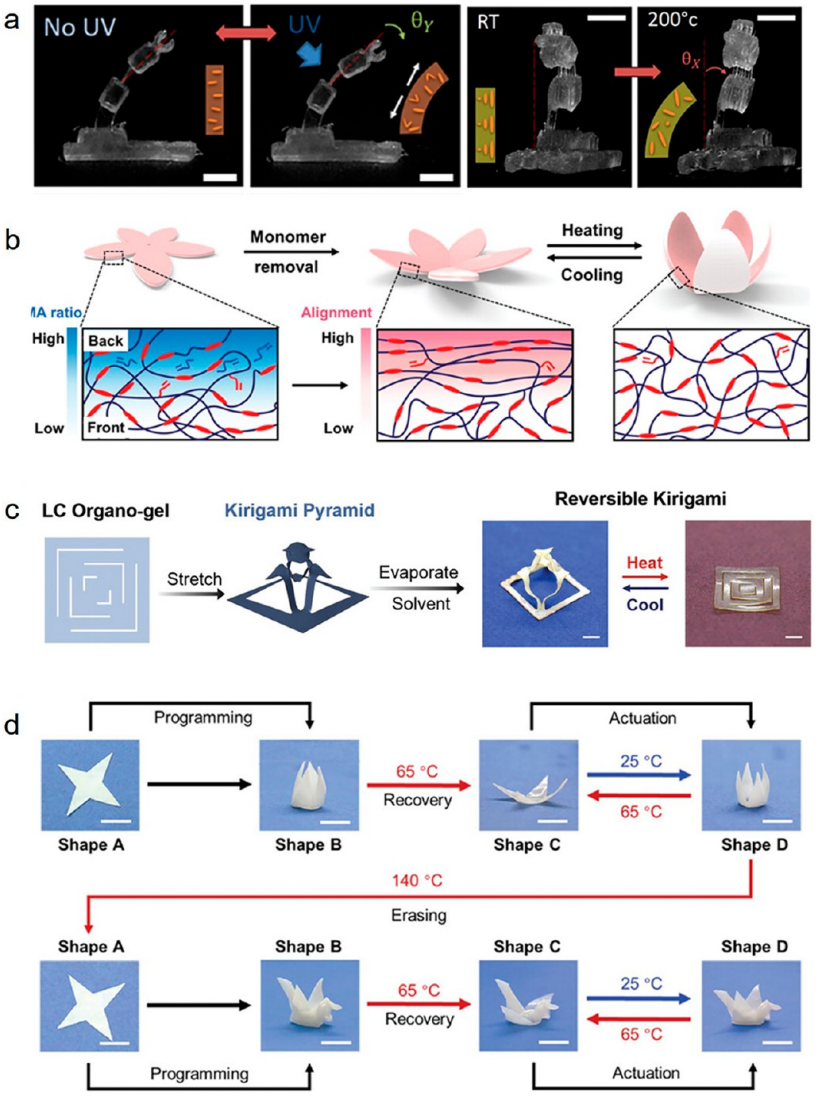

Figure 9. LCEs fabricated by DLP printing. (a) Multi-responses of an LCE robotic arm.[119] Reproduced with permission. Copyright 2019, American Chemical Society. (b) Biomimetic petal-like LCE structure exhibiting reversible actuations.[121] Reproduced with permission. Copyright 2021, John Wiley & Sons, Inc. (c) DLP printed LCE actuator with topological structure.[122] Reproduced with permission. Copyright 2021, John Wiley & Sons, Inc. (d) DLP printed LCE origami actuator.[123] Reproduced with permission. Copyright 2022, John Wiley & Sons, Inc.

4D-printed LCEs were successfully obtained. These 4D-printed LCE splines could be cyclically and reversibly changed between various shapes, demonstrating good actuation performance (Figure 7d).

Furthermore, dynamic bonds enhance the deformability of 4D printed LCEs.[71,98,100,113] For example, Lu et al. used UPy supramolecular interactions, dynamic Diels-Alder (DA) cross-linking, and azobenzene to achieve the 3D printing of optically controlled LCE structures, which could maintain long-term retention of a deformed state[71] (Figure 7e). Upon heating to 130 °C, the UPy dimer dissociates and the furan-maleimide adduct is activated, resulting in the de-cross-linking of the LCE and the decrease in viscosity. This allows the liquid crystal ink to be extruded through DIW and aligned in the printing direction. Subsequently, with the re-formation of DA and hydrogen bonds, the oriented structure is fixed. The UPy supramolecular cross-linked structure is temporarily disrupted under UV light irradiation and rapidly re-formed after UV light removal, resulting in the "locking" of the deformed structure, which can be recovered after heating.

Currently, most of the LCE structures printed with DIW technology are still mainly 1D fibers or 2D films, while the fabrication of more complex 3D actuator structures remains a significant challenge, this is primarily attributed to the limitations in *z*-axis orientation. Nonetheless, the combination of active LCE materials and passive support materials offers a promising approach for the construction of 3D LCE actuators[108] (Figure 7f). Recently, the preparation of 3D LCEs has also been achieved by extruding the LCE ink into the gel matrix using DIW printing.[114]

4.1.2. TPP-DLW. Due to its nonlinear absorption process of two-photon polymerization in direct laser writing, the polymerization will only occur at the two-photon focus area, providing the highest printing accuracy among all printing methods. This approach allows for a wide range of scales, from the nanometer to the micrometer, making it a potent technique for fabricating structures with arbitrary geometry and high resolution. LCEs with microstructure can be produced by the TPP-DLW method, and their molecular arrangement can be controlled at the submicron scale by the surface templating method. The LC

https://doi.org/10.1021/cbe.4c00027
Chem Bio Eng. 2024, 1, 488−515

elements can be adjusted in any direction by moving the laser focus position. Nevertheless, the preparatory steps before printing and the orientation process of the LC usually extend the overall printing duration. Zeng et al. fabricated LCE structures with submicron resolution by TPP-DLW printing,[115] and the alignment of the liquid crystal elements was achieved through surface friction (Figure 8a). The materials utilized in TPP-DLW comprise photopolymerizable acrylate LC monomers, azobenzene dyes, crosslinkers, and photoinitiators. Following the injection of the ink into the uniaxial friction polyimide-coated glass, orientation is achieved by surface friction and polymerization is subsequently initiated by laser scanning.

Then, to create miniature LCE actuators, the research team used micro-grating patterns instead of unidirectional friction surfaces to align the mesogens, achieving control at the molecular scale. The printed structures can be deformed in various directions according to the micrograting orientation, resulting in complex actuation modes. In addition, continuous and discontinuous pixelated channels can be produced with the advantage of the high-resolution characteristic of TPP-DLW printing, therefore enabling the creation of 2D and 3D oriented structures with resolutions up to 5 μm.[77] Using selective photopolymerization, microstructures with identical geometries can exhibit distinct deformation behaviors, due to different orientation fields (Figure 8b). Guo et al. presented an interesting illustration of LCE microstructure fabrication using the TPP-DLW technique.[116] Using surface friction, they fabricated LCE cubes with arbitrary mesogen orientation. These cubes are subsequently assembled into 3D structures such as lines, grids, or skeletal frameworks to obtain diverse geometries with different orientation structures, enabling complex shape transformations and anisotropic physical properties (Figure 8c).

Moreover, gold nanorods,[117] multi-walled carbon nanotubes, and graphene oxide[118] have also been incorporated into the printable LC inks, thus providing LCEs with enhanced versatility, such as improved mechanical properties and light responsiveness (Figure 8d & 8e).

4.1.3. DLP. DLP technology employs a digital micromirror device (DMD) to project the 2D cross-section pattern of the printed model on the surface of a liquid resin in the form of ultraviolet light to induce polymerization, enabling the gradual layer-by-layer curing of the resin upon exposure to the light. The resolution of DLP can reach micron level. Compared to the TPP-DLW relying on surface treatment orientation, DLP has a broader range of orientation modes. Tabrizi et al. combined a rotatable magnetic field with DLP to regulate material composition and molecular orientation at each solidified layer, thereby building hierarchical properties of structure and function.[119] The thermal and light-responsive LCEs were used to construct a multi-response robotic arm, and various segments of the arm exhibited distinct orientation characteristics and response capabilities (Figure 9a). Li et al. used the shearing action generated by the cyclic rotation of the resin tray to induce the orientation of liquid crystal elements throughout the layer-by-layer printing process.[120] This approach significantly reduces the printing time compared to DIW, and the prepared photocuring actuator can bend in response to thermal stimulation. By combining the micro-photoelectric element with the bending actuator, the bending deformation of the actuator can be detected by the optical sensor. In addition to orienting mosegen units during the printing process, evaporation of unreacted monomers or solvents can also be used for the alignment of mosegen elements. When DLP is used to print thicker samples, there will be unreacted monomers with a gradient content in the printed product due to the attenuation of light. During the process of removing these monomers at high temperatures, the difference in volume contraction of the object will induce the production of the original alignment, resulting in reversible bending motion[121] (Figure 9b). Similarly, Jin et al. reported that solvent evaporation under stress can be used for mesogen unit arrangement in isotropic LCN gels, which may be related to the micropores generated during the volume shrinkage process.[122] The LC orientation can be repeatedly established and erased through the process of solvent evaporation and subsequent re-swelling (Figure 9c). Recently, Chen et al. reported a strategy for reversibly locking and unlocking orientation after printing using physical phase transitions (crystallization and melting).[123] Similar to the process of solid-state shaping, they designed a liquid crystal network with two phases where orientation can be induced through mechanical forces at high temperatures and then secured through crystalline formation. Subsequently, a reversible shape change occurred due to the liquid crystal phase transformation (Figure 9d). The orientation of the LCEs could be erased by melting the crystalline region to enable a new round of programming.

4.1.4. MEW. High-precision manufacturing of programmable LCE microfibers has always been a challenge. MEW printing technology is a low-cost, large-scale, and high-resolution manufacturing technology that has advantages in the preparation of ultra-fine LCE fibers.[124] The MEW printing technology employs a high-voltage (2 to 3 kV) electric field applied between the metal needle and the substrate to generate LCE Taylor cones and microfibers, which are then deposited onto the substrate to fabricate various cross-scale 3D structures. Due to the high shear force inside the Taylor cone, the LC mesogens undergo orientation within the structure and the LCEs are obtained by photo-crosslinking. This technique was first reported in 2022 by Carlos et al, who fabricated LCE fibers with a diameter of tens of microns using this method[124] (Figure 10a). After that, Lu's research group used this technique to fabricate a range of LCE

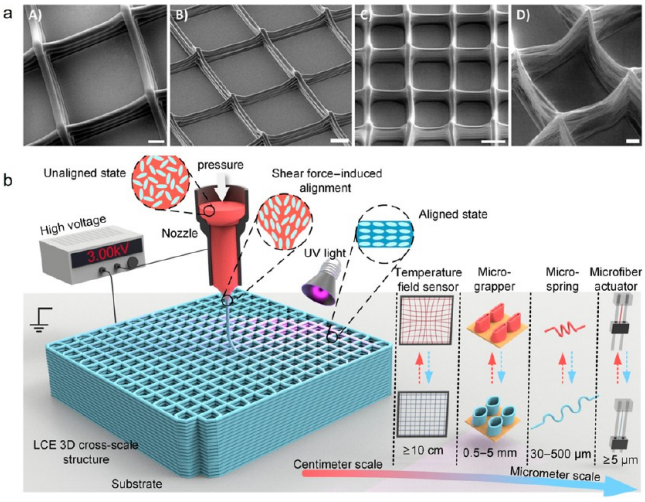

Figure 10. LCEs fabricated by MEW printing. (a) MEW printing LCEs 3D structures.[124] Reproduced with permission. Copyright 2022, John Wiley & Sons, Inc. (b) Multifunctional LCEs fabricated by MEW printing.[125] Reproduced with permission. Copyright 2024, American Association for the Advancement of Science.

https://doi.org/10.1021/cbe.4c00027
Chem Bio Eng. 2024, 1, 488−515

Table 2. Overview of the 4D Printed LCE Methods: Printing Types, Alignment Methods, Reaction Mechanism, Ink Compositions, and References[a]

Printing type	Alignment methods	Reaction mechanism	Ink components	References
DIW	Rheological alignment	Radical polymerization	RM: BHHBP Chain extender: 6HCA Cross-linker: PSA Photoinitiator	56
DIW	Rheological alignment	Amino Michael Addition	RM: RM82/BIP Cross-linker: 1,5-diaminopentane	42
DIW	Rheological alignment	Amino Michael Addition	RM: RM82 Chain extender: 5-Aminopentanol/ Furan-2-ylmethanamine Cross-linker: Bismaleimide/Upy-NCO Photoinitiator	71
DIW	Rheological alignment	Amino Michael Addition	RM: RM82 Chain extender: *n*-butylamine Photoinitiator	94, 95, 99, 103, 109, 126, 127
DIW	Rheological alignment	Amino Michael Addition	RM: RM257 Chain extender: *n*-butylamine Photoinitiator	101, 128−130
DIW	Rheological alignment	Amino Michael Addition	RM: RM82 & RM257 Chain extender: N,N-dimethylpropane-1,3-diamine Photoinitiator	131
DIW	Rheological alignment	Thiol-Michael addition	RM: RM82 Chain extender: *n*-butylamine Cross-linker: TATATO	35
DIW	Rheological alignment	Thiol-Michael addition	RM: RM82 & RM257 Chain extender: GDMP/EDDET/PDT Cross-linker: TATATO	104
DIW	Rheological alignment	Thiol-Michael addition	RM: RM257 Chain extender: EDDET Photoinitiator	102, 106, 111, 132, 133
DIW	Rheological alignment	Thiol-Michael addition	RM: RM82 Chain extender: 1,5-diaminopentane Cross-linker: 1,5-diaminopentane Photoinitiator	105
DIW	Rheological alignment	Thiol-Michael addition	RM: RM257 Chain extender: EDDET Cross-linker: PETMP	107, 134
DIW	Rheological alignment	Thiol-Michael addition	RM: RM82 & RM257 Chain extender: EDDET Photoinitiator	108
DIW	Rheological alignment	Thiol-Michael addition	RM: RM82 & RM257 Chain extender: BDMT Photoinitiator	112
DIW	Rheological alignment	Thiol-Michael addition	RM: RM82 & RM257 Chain extender: EDDET Photoinitiator	135, 136
DIW	Rheological alignment	Thiol-Michael addition	RM: RM257/LC756 Chain extender: EDDET Photoinitiator	137
DIW	Rheological alignment	Thiol-Michael addition	RM: RM82 Chain extender: EDDET Photoinitiator	138
DIW	Rheological alignment	Thiol-Michael addition	RM: RM82 & RM257 Chain extender: *n*-butylamine EDDET Cross-linker: TATATO	139
DIW	Rheological alignment	Thiol−isocyanate reactions	RM: RM82 & RM257 Chain extender: HDI/EDDET Photoinitiator	100, 113

https://doi.org/10.1021/cbe.4c00027
Chem Bio Eng. 2024, 1, 488−515

Table 2. continued

Printing type	Alignment methods	Reaction mechanism	Ink components	References
TPP-DLW	Photopatterned surface-enforced alignment	Radical polymerization	RM: C6BP & RM257 Photoinitiator	77, 115, 116, 118, 140
DLP	Magnetic field-assisted alignment	Radical polymerization	RM: RM257/Azo-2 Photoinitiator	119
DLP	Rheological alignment	Thiol-Michael addition	RM: RM82 & RM257 Chain extender: EDDET Cross-linker: TATATO Photoinitiator	120
DLP	Solvent evaporation	Radical polymerization	RM: RM82 Photoinitiator	121
DLP	Solvent evaporation	Thiol-Michael addition	RM: RM82 Chain extender: PDT Photoinitiator	122
DLP	Mechanical alignment	Thiol-Michael addition	RM: RM82 Chain extender: PEGDA/EDDET Cross-linker: PETMP Photoinitiator	123
DLP	Mechanical alignment	Thiol-Michael addition	RM: RM82 Chain extender: EDDET Cross-linker: TATATO Photoinitiator	141
MEW	Rheological alignment	Amino Michael Addition	RM: RM82 Chain extender: *n*-butylamine Photoinitiator	124
MEW	Rheological alignment	Amino Michael Addition	RM: RM257 Chain extender: EDDET Photoinitiator	125

[a]Photoinitiators are not specifically categorized in this review. RM: reactive mesogens.

soft actuators from micrometer to centimeter scale through layer deposition.[125] The LCE fiber actuator is applied to temperature field detection, and an environmental temperature field sensor that integrates machine vision and deep learning models is developed for the first time (Figure 10b).

As mentioned above, we have briefly illustrated the equipment, the principle and the latest advances in 4D printing of LCEs. To achieve a reversible shape change, the orientation of the LC elements needs to be aligned before the cross-linking process. For DIW and MEW printing, LC orientation is primarily achieved through the shear stress and tensile stress applied during the extrusion and printing processes, while for 2PP and DLP printing, the LC alignment is mainly achieved by the magnetic field and the surface orientation. In general, the 4D printing ink of LCEs mainly focuses on the Michael addition reaction between amine or thiol with acrylate. Therefore, in Table 2 and Figure 11, we summarize the printing method, orientation method and ink composition of 4D printed LCEs.

The chemical structures of the monomers and other compounds in Table 2 are shown in Figure 11.

4.2. The Relationship among the LCEs, the Printing Methods, the Orientation/Structure, and the Shape-Morphing Properties. In summary, the type and the printing method of 4D printed LCEs determine the orientation and structure of the LCEs and then affect the deformation characteristics of the LCEs. Here, the relationship among the LCEs, the printing methods, the orientation/structure, and the shape-morphing properties were discussed in detail.

(1) Based on the stimulation, 4D printed LCEs can be classified into thermoresponsive, light-responsive, electric-field-responsive, magnetic-field-responsive, and moisture-responsive LCEs. From the perspective of materials chemistry, thermoresponsive LCEs are fabricated by radical polymerization, amino-Michael addition, thiol-Michael addition and thiol-isocyanate reaction. Radical polymerization is completed by direct polymerization of acrylate groups. Amino-Michael additions and thiol-Michael additions between acrylate monomers and amines or thiols afford the LC oligomers, which are further cross-linked by heat or light to form the LCEs. LCEs based on thiol-isocyanate reaction are obtained by cross-linking with after chain extension. Light-responsive LCEs can be divided into two types, the one is formed by incorporating photo-switches into the LCE network structure, and the other is obtained by adding photothermal dyes/particles into polymer matrix. Electrically and magnetically responsive LCEs are fabricated by functionalization with conductive and magnetic fillers, respectively. Moisture-responsive LCEs are fabricated by incorporating hygroscopic groups into the LCE networks.

(2) The orientation structure or profile of the mesogens in LCE actuators is most important because it determines the deformation of LCEs. Traditional orientation methods for LCEs, such as mechanical alignment or surface friction, typically can only produce uniform orientation structures, showing simple shrinkage or bending deformation. Although the external field (light, electric field and magnetic field) assisted orientation can create more complex orientation structures, the prepared actuators are usually limited to thin films. 4D printing enables precise and convenient control of the orientation

https://doi.org/10.1021/cbe.4c00027
Chem Bio Eng. 2024, 1, 488−515

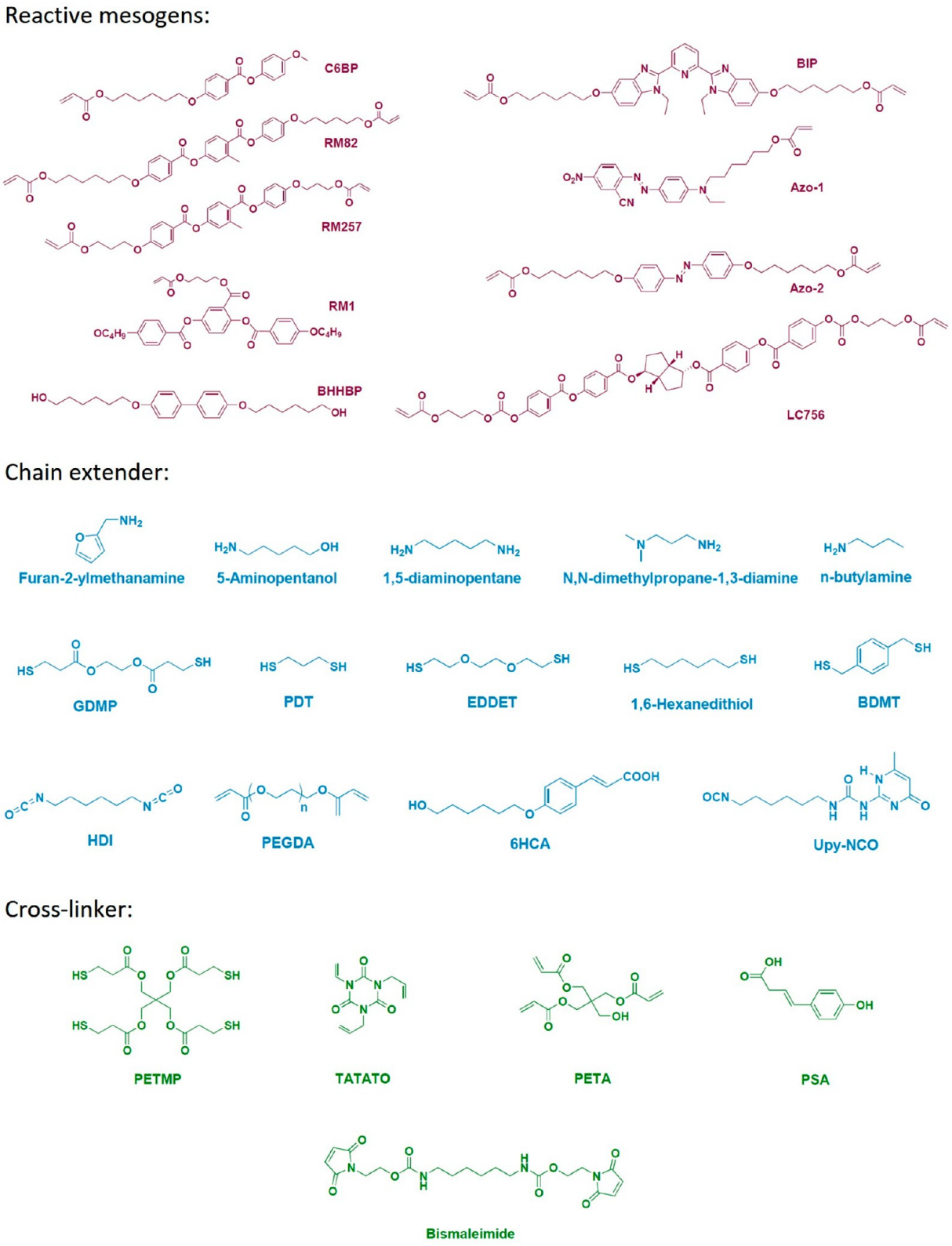

Figure 11. Chemical structures of the compounds involved are in Table 2.

of liquid crystal units and the macro shape of the actuator, resulting in complex and changeable deformation patterns.

The four common printing methods have their own applications and inherent limitations. For DIW printing technology, the mesogen units will be oriented along the printing path, and a same shape may have different deformation modes due to different printing paths. However, this method has certain requirements for the rheological properties of the ink, and the orientation is typically constrained to the x-y axis plane. Therefore, LCEs prepared by DIW are usually 1D fibers or 2D planar

https://doi.org/10.1021/cbe.4c00027
Chem Bio Eng. 2024, 1, 488−515

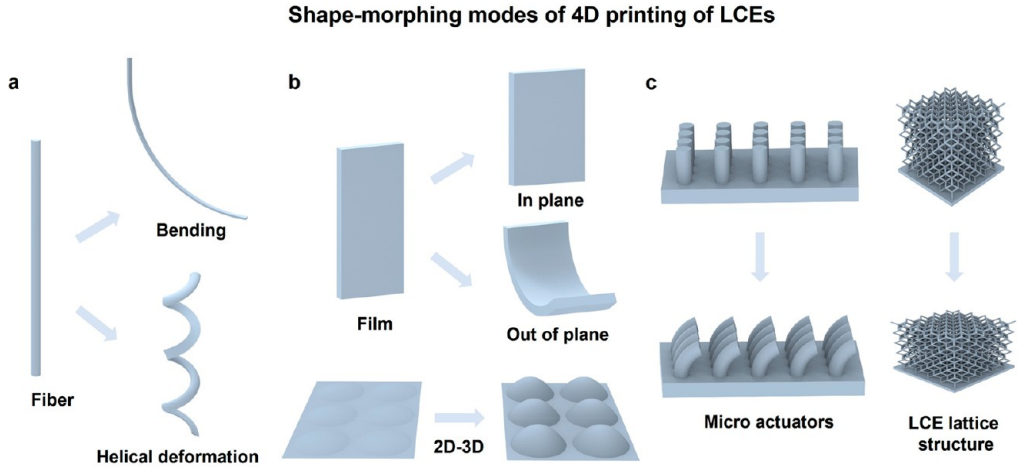

Figure 12. Shape-morphing modes of 4D printed LCEs with (a) 1D structure, (b) 2D structure, and (c) 3D structure.

films, and it is difficult to print LCEs with complex 3D structures by this method. The photocuring printing method DLP requires the photosensitive resin to have a low viscosity and the capacity for rapid crosslinking under ultraviolet light irradiation. TPP-DLW which has high resolution and can fabricate arbitrary 3D shapes and alignment in the *Z*-axis direction, is an ideal way to manufacture micro-actuators, but the orientation and fabrication of microstructures will be time-consuming, and the manufacture of actuators with high precision and large size also needs further exploration. MEW printing has advantages in the preparation of ultrafine LCE fibers but needs specifically home-designed equipment. Despite various challenges and issues, 4D printing has promoted the manufacturing and application of LCE actuators to a new level.

In addition, the 4D printing method can also make LCEs easily composite with other materials, such as LCEs with different T_{NI} or response characteristics, or inorganic carbon materials like carbon nanotubes, carbon fibers, or metal fillers like gold nanorods, ferromagnetic particles, etc. Special printing methods can also be used to achieve the combination of different materials within spatial structures, such as core-shell structures or hinge structures. Undoubtedly, these advancements significantly enhance the deformation capabilities of LCE actuators, expanding their range of potential applications.

(3) Shape-morphing properties. In Figure 12, we have summarized the deformation mode of 4D printed LCEs based on 1D, 2D, and 3D LCE structures.

The deformation mode of the printed 1D structure LCE fiber is depended on its cross-section structure. LCE fiber with symmetric circular cross-section tends to display bending deformation[143] while the fiber with asymmetric cross-section tends to show spiral deformation[42] (Figure 12a). Based on this, LCE fibers have been reported to mimic soft robots. In addition, more complex deformation is often generated by combining LCE fibers with mechanical devices, such as robotic arms. The deformation modes of planar LCEs include in-plane contraction, out-of-plane bending, and 2D-3D deformation (Figure 12b). In-plane contraction usually occurs in structurally symmetric LCEs, while out-of-plane contraction often takes place in structurally asymmetric LCEs or bilayer composites composed of LCEs and other materials.[144] In addition, LCEs with specially designed mesogen orientation can undergo 2D-3D deformation when subjected to external stimuli.[71] 3D LCE structures are often fabricated by DLP printing or TPP-DLW printing. LCE lattice structures often exhibit overall shrinkage when stimulated.[145,146] The LCE microactuators often undergo deformation such as bending or rotation upon exposure to stimuli[147] (Figure 12c).

In conclusion, 3D and 4D printed shape-morphing LCEs have been significantly developed over the past decade. By introducing functional dopants, the responses of LCEs have been expanded from the initial thermal responsiveness to optical, electric, and magnetic responsiveness.[142] The printing methods also include DIW, DLP, TPP-DLW, and MEW. The structures of 4D printed LCEs have developed from single-layer structures to multi-layer structures, and from flat 1D arrangements to intricate 3D topologies. These advancements have greatly increased the range of applications of 4D printed LCEs. In summary, the printing method of 4D printed LCEs determines the orientation and structure of the LCEs and then affects the deformation characteristics of the LCEs. Here, we summarize the applications of 3D and 4D printing of shape-morphing LCEs in Table 3, which include the printing methods, function dopants, printing structures, stimuli, and actuation modes.

5. APPLICATIONS OF 4D PRINTING OF LIQUID CRYSTAL ELASTOMERS

LCEs have great application potential as soft smart materials because of their remarkable ability to achieve substantial and reversible deformations. However, to realize the shape transformation, it is essential to orient the liquid crystal units and fix the orientation structure through crosslinking to prepare monodomain LCEs. As mentioned above, the traditional preparation methods, such as the "one-step method" and the "two-step method", have some inevitable limitations, due to not only the complexity of the preparation process but also the difficulty in designing the oriented structure and deformation structure. The emergency of 4D printing not only streamlines the manufacturing process of LCEs but also expands the application range of LCEs in the field of soft smart materials. 4D-printed LCEs offer more possibilities for creating new LCE devices that are programmable, stimuli-responsive, and possess ideal geometries. As a result, it has great application prospects in soft robots, bionic actuators, energy dissipators, microfluidic devices, light-responsive devices, cell culture and so on. In this

https://doi.org/10.1021/cbe.4c00027
Chem Bio Eng. 2024, 1, 488−515

Table 3. Summary of the Applications of 3D and 4D Printed Shape-Morphing LCEs

Printing methods	Functional dopants	Printing Structures	Stimuli	Actuation modes	References
DIW	Fumed silica	Bilayer hinge structure	Heat	Folding and unfolding	35
DIW		Bilayer controllable orientation gradient structure	Heat	Bending	56
DIW		LCE artificial tendril and flagellum	Heat	Spiral deformation	42
DIW		Flower-like and braille-like actuators	UV light	Bending	71
DIW		Layered spiral disk actuator, mesh porous actuator and conical array actuator	Heat	Shrinking and bulging	95
DIW		LCE-PDMS variable focus lens	Heat	Shrinking and bulging	99
DIW		One-layer archimedean chord print pattern, bilayer rectangular LCE film and porous structure	Heat	Shrinking and bulging	94
DIW	Liquid metal	Monolithic structures	Electricity and NIR light	Bending	101
DIW	Liquid metal	Coaxial LCE (shell)-LM (core) fiber	Electricity	Shrinking and bulging	103
DIW		Disk and alternate porous structures	Heat	Shrinking and bulging	104
DIW		Flower-like actuators and active auxetic lattice structures	Heat	Twisting, bending and shrinking	102
DIW		Helix of the disc structure	Heat	Twisting and bulging	105
DIW		Honeycomb and spiral director structures	Heat and UV light	Shrinking, bulging, and twisting	100
DIW		Stipes structure	Heat	Bending	113
DIW		Soft pneumatic actuators	Gas	Elongation, bending, and twisting	106
DIW		LCE fiber	Heat	Shrinking and lifting	107
DIW		3D spatial LCE lattices	Heat	Shrinking	108
DIW	MWCNTs	Fully soft robotics	NIR light	Twisting and swimming	109
DIW	TiNC	Origami-inspired structure	NIR light	Bending	111
DIW	Aramid fibers	Off-center LCEs fiber	Heat	Twisting	112
DIW	NdFeB microparticles	Four-petal magLCE flower and strip robot	Magnetism and heat	Twisting, crawling, rolling and twirling	139
DIW	Liquid metal	LCE crawler with an on/off photoresistor	Heat	Crawling	128
DIW		Tubule robot	Heat	Spiraling and rolling	126
DIW	Perylene diimide	Bimorph actuators and spiral actuators	NIR light	Bending and bulging	127
DIW	Liquid metal	Biomimetic sea turtle actuator	Heat	Crawling	135
DIW	SMP	LCE-SMP composite wrench	Heat	Shrinking	136
DIW	Fluorescent dye	LCE-PEI bilayer structure	365 nm UV light	Bending	138
DIW	(PQDs)	Scroll structure	Heat	Unfolding	130
TPP-DLW		Microrings and woodpile structure			115
TPP-DLW		Cylindrical structure and stripe structure	532 nm blue light	Twisting	140
TPP-DLW		Films, rings, and spiral coils	Solvent	Twisting	77
TPP-DLW		Cuboid and rectangular LCE frame	Heat	Folding, unfolding and bending	116
TPP-DLW	AuNRs	Woodpile structures, hexagonal photonic crystal structures, frame structures and micro clamp structures	NIR light	Shrinking	117
TPP-DLW	MWCNTs, GO and AuNRs	Woodpile structure, regular dodecahedron, octahedron, pentagon cylinder, and micro-clamps	UV Light	Shrinking	118
DLP		Pyramid structure, hatch-patterned suspensory structure, and light-responsive array of microstructures	Heat and UV light	Bending	119
DLP		Soft robotic gripper, soft maneuvering robot and optomechanical self-sensing sensor	Heat	Grasping, lifting, crawling and bending	120
DLP		Biomimetic flowers and strips	Heat	Twisting, curling and bending	121
DLP		Origami crane and kirigami pyramid	Heat	Folding, unfolding and bulging	122
DLP		Four-pointed star, origami crane and other complex geometries structures	Heat	Bending and flapping	123
DLP	Azobenzene dye, IR-780 dye and sudan blue II dye	Bilayer LCE actuators	Heat	Bending	141
MEW		Ultrafine LCEs fiber	Heat	Shrink	124
MEW		Ultrafine LCEs lattice and flytrap actuator		Shrink	125

https://doi.org/10.1021/cbe.4c00027
Chem Bio Eng. 2024, 1, 488−515

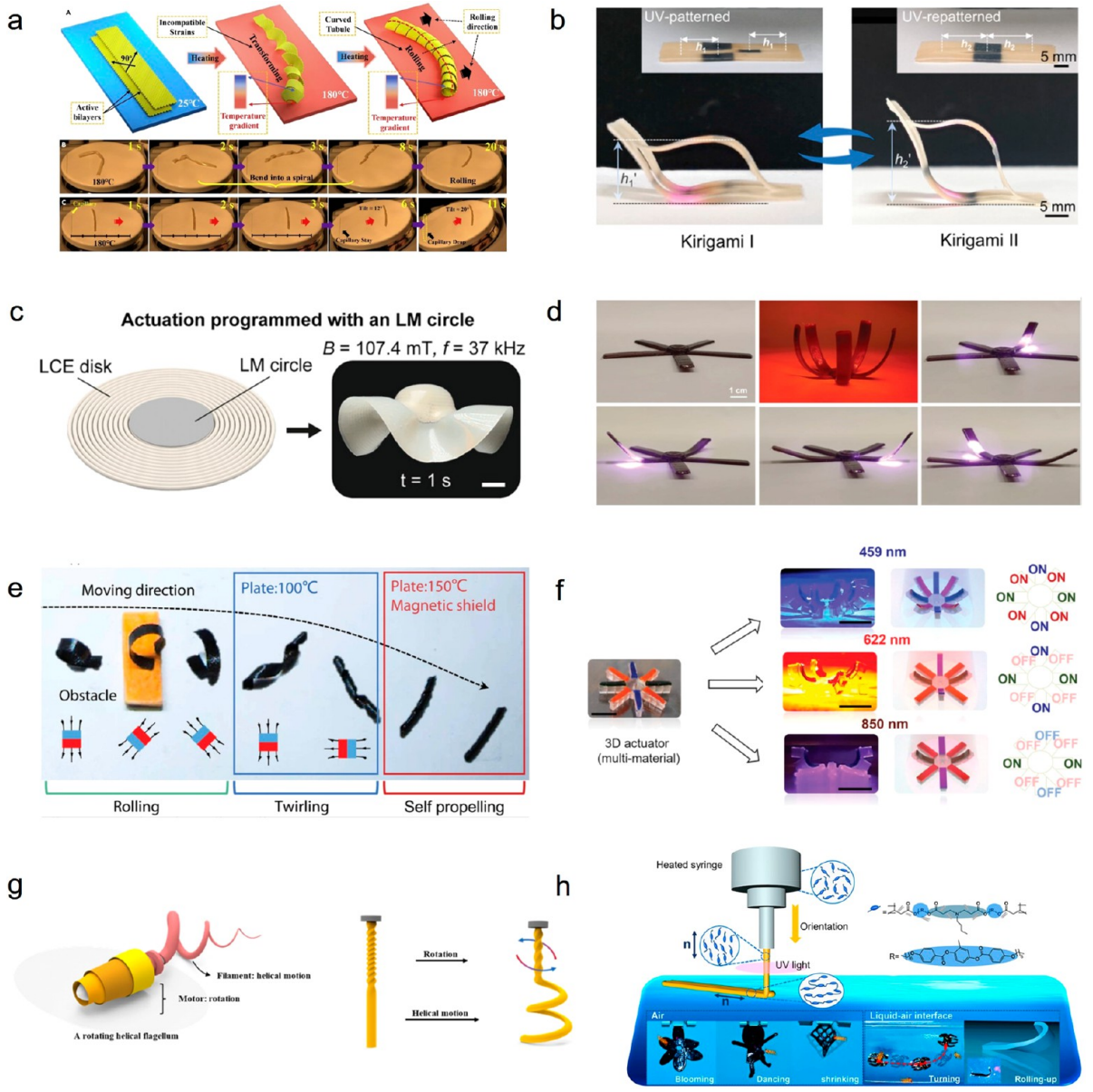

Figure 13. Applications of 4D printed biomimetic LCE soft robots. (a) The LCE-based soft robot is capable of autonomous walking.[126] Reproduced with permission. Copyright 2021, Elsevier. (b) 4D printed nanocrystals/LCE composite actuators.[111] Reproduced with permission. Copyright 2023, John Wiley & Sons, Inc. (c) LCE-liquid metal (LCE-LM) composite actuators.[135] Reproduced with permission. Copyright 2023, John Wiley & Sons, Inc. (d) AuNR/LCE composite actuators.[110] Reproduced with permission. Copyright 2023, John Wiley & Sons, Inc. (e) Magnetic field responsive LCE strip robots.[139] Reproduced with permission. Copyright 2023, John Wiley & Sons, Inc. (f) Multi-wavelength responsive LCE composite actuators.[141] Reproduced with permission. Copyright 2023, John Wiley & Sons, Inc. (g) LCE artificial tendrils showing evolutionary biomimetic locomotion.[42] Reproduced with permission. Copyright 2023, John Wiley & Sons, Inc. (h) Photoresponsive 3D-printed carbon nanotube/LCE composite soft robotics.[109] Reproduced with permission. Copyright 2022, American Chemical Society.

section, we provide a comprehensive overview of the current research landscape surrounding the applications of 4D printed LCEs, addressing existing challenges, and outlining future development directions in this field.

5.1. Biomimetic Soft Robots. In recent decades, various types of soft actuators have emerged, encompassing pneumatic actuators, hydraulic actuators, ion exchange polymers, metal/polymer composites, dielectric elastomer actuators, hydrogels, and LCE actuators.[148−150] Compared with traditional robots, soft robots have potential advantages in improving the safety, environmental adaptability and continuous deformation for human-computer interaction.[151−153] Because of their large reversible strain and programmable deformation properties, LCEs exhibit immense potential in the development of soft robots.[36,59,154−157] To provide soft robots with multifunctionality and precise control over complex actions, considerable research efforts have been dedicated to the exploration of 4D printed LCEs soft robots.

Heat treatment stands out as the most prevalent stimulus, and monodomain LCE actuators are prepared by temperature-controlled thermal transitions between liquid crystal and isotropic phases of the materials. Since 2017, when the Ware research group first reported the direct printing of LCEs via DIW, the inks and methods for printing LCE in 4D have made significant progress. Zhai et al. fabricated an LCE soft robot capable of autonomous walking[126] (Figure 13a). This robot was

https://doi.org/10.1021/cbe.4c00027
Chem Bio Eng. 2024, 1, 488−515

fabricated by the DIW printing method and capable of thermal actuation and cordless rolling. Upon heating to above 160 °C, the printed rectangular LCE transforms into a small tube and autonomously initiates rolling on the heating plate. The speed of the robot can be modulated by adjusting the size of the LCEs. This feature enhances the robot's tactile perception, enabling it to navigate and explore obstacles in its advancing path. This small tubular actuator provides loading space, which can be used for transportation. Therefore, the robot is expected to be used in extreme environments, such as high temperatures exceeding 200 °C or tight spaces.

Recently, silver ink,[50] carbon nanotubes (CNTs),[109] gold nanorods (AuNRs),[110] nanocrystals,[111] magnetic nanoparticles,[139] and liquid metals[128] have been incorporated into LCE printing inks, significantly enhancing the actuation performance of LCEs, and the actuation modes have also been extended to optical and magnetic actuation and so on.[85,158] The representative works are described below. Recently, nanocrystals have also been incorporated into 4D-printed LCEs, offering huge opportunities for creating stimuli-responsive actuators. This composite ink is capable of reprogrammable photochromic and photoactivated responsiveness. Chen et al. recently fabricated titanium dioxide nanocrysts (TiNC)/LCE composite actuators by DIW printing.[111] Under near-infrared light irradiation, the temperature of the actuators increases rapidly due to the photothermal effect, exhibiting good actuation ability, which can imitate mechanical grasper and other movements (Figure 13b). In addition, they also printed a series of topological LCE actuators through DIW. This research offers a new insight for the design of unique and tunable multifunctional adaptive actuator structures, and has potential applications in intelligent building engineering, camouflage, multilevel information storage, etc. Maurin et al. reported a novel LCE-liquid metal (LCE-LM) composite actuator that is capable of ultra-fast actuation[135] (Figure 13c). This actuator comprises liquid metal enclosed between two layers of LCEs. The incorporation of liquid metal endows the actuators with remote actuation capability. The LCEs actuator is fabricated by DIW printing, allowing precise control over its actuation mode by manipulating the printing path. Wang et al. developed a 3D printed photoresponsive gold nanorods (AuNRs) /LCE composite that allows photothermal actuation of printed devices at extremely low AuNRs concentration (0.1 wt %)[110] (Figure 13d). Sun et al. developed a magnetic LCE ink by dispersing ferromagnetic particles within an LCE matrix.[139] This magnetic LCE ink can be printed by a customized DIW printing platform to create an anisotropic magnetically responsive device. The magnetic LCE strip robot exhibits complex shape-morphing capacity, which includes crawling, rolling, twirling, and self-propelling (Figure 13e).

Visible light-driven LCEs are the future development tendency. LCEs containing photoresponsive groups have shown significant potential in remotely controlled soft robots. However, their implementation primarily relies on azobenzene groups and requires the use of ultraviolet light, which is, to some extent, harmful to both human health and the surrounding environment. Montesino et al. prepared a 4D printed LCE ink containing green-light absorbing perylene diimide chromophores, enabling the fabrication of a photoactive LCE actuator through direct ink writing.[127] Upon green light illumination, the LCE undergoes photothermal actuation and simultaneously generates new absorption bands in the far-red and near-infrared regions, which can be attributed to the formation of free radicals. Mechanical actuation is triggered by far-red light radiation, and notably, the original absorption spectrum can be restored during this process. This material strategy, which uses green and far-red light to avoid the harmfulness of ultraviolet light, shows great potential for the future development of reconfigurable actuators in biomedical applications. Due to the high spatial resolution, DLP has recently shown advantages in 4D printing of complex LCE structures. Mainik et al. reported a general method for the first time to fabricate a DLP-printed multi-responsive LCE actuator based on a double-layer structure that exhibited reversible and complex actuation modes.[141] These structures are composed of an active layer made of LCE and a passivation layer made of a printable non-responsive elastomer. Multi-wavelength responsiveness is easily achieved by incorporating diverse organic dyes that exhibit absorption in different regions, ranging from visible blue to the near-infrared spectral range. Finally, they used DLP printing to create a double-layer complex 3D structure composed of four different materials (one passive material and three different LCE active materials), which was able to perform three different bending modes on demand by exposing it to different wavelengths of light (Figure 13f).

Learning from organisms in nature and imitating their behaviors has been an important research direction for materials scientists. For example, there are a lot of spiral phenomena in nature. However, how to simulate this behavior has always posed a challenge for materials scientists. Our research group has successfully simulated this behavior by using DIW-printed LCE fiber actuators.[42] Specifically, the DIW-printed LCE fibers exhibit different orientation degrees between the core and skin. Upon heating, the spiral actuation occurs naturally due to the different driving forces on the core and skin of the LCE fiber. To endow this spiral actuator with versatile actuation behavior, we introduce the metal-ligand dynamic bond into the system, which endows the LCE actuators with reconfigurable functions. Reconfigurable soft actuators can be programmed to respond differently to the same stimulus, and exhibit significant potential for enhancing the adaptability of actuation. Through reconfiguration at high temperatures, the helical LCE actuators can accomplish actions such as left and right rotation. Finally, based on the dynamic feature of the metal-ligand coordination, we successfully reprogrammed the LCE fiber actuators capable of simultaneous rotation and coiling, which can mimic the movement of flagellar (Figure 13g). Finite element simulations are well consistent with the experimental results.

Soft robot movements at the liquid-gas interface are becoming increasingly important for intelligent societies. Nonetheless, current soft robot motions are constrained to two dimensions. Because of the imbalanced mechanical conditions, achieving 3D motions at the liquid-gas interface remains a major challenge. Inspired by a meniscus reptile, Wang et al. developed a photoresponsive 3D-printed CNTs/LCE composite soft robot.[109] The robot could be remotely actuated with light, allowing for precise spatiotemporal control, enabling the expansion of the application range, for example, a controlled movement of the LCE robot within a closed tube (Figure 13h).

5.2. Mechanical Devices. LCE actuators can be designed into various micro-mechanical devices because of their multi-stimuli response and convenient preparation methods.[149,159−162] The LCE mechanical device is a device that converts the external input energy to drive the movement of the device.[163] 4D printing technology not only simplifies the manufacturing process of traditional LCE actuators, but also

https://doi.org/10.1021/cbe.4c00027
Chem Bio Eng. 2024, 1, 488−515

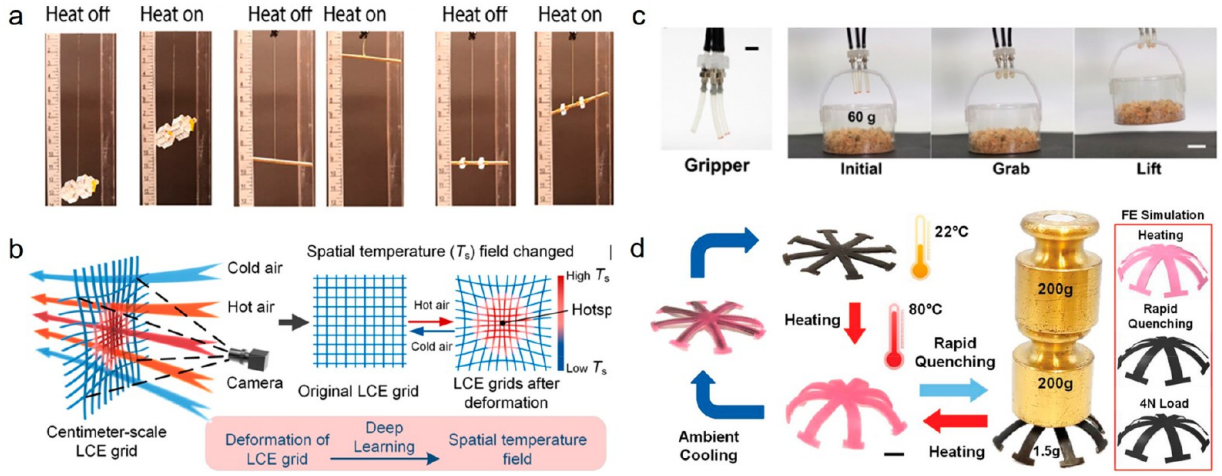

Figure 14. Applications of 4D printed micro-mechanical device. (a) DIW printed LCEs fiber that can lift heavy objects.[143] Reproduced with permission. Copyright 2024, John Wiley & Sons, Inc. (b) MEW printed LCEs fiber actuator was applied to temperature field detection.[125] Reproduced with permission. Copyright 2024, American Association for the Advancement of Science. (c) LCE-SPA actuator displaying grasping actions.[106] Reproduced with permission. Copyright 2023, The Royal Society of Chemistry. (d) LCE/SMP composite actuator. Reproduced with permission.[136] Reproduced with permission. Copyright 2022, John Wiley & Sons, Inc.

has significant advantages in the design of micro-mechanical LCE devices with complex structures.

LCE fibers fabricated by DIW or MEW printing have played an important role in robotic arms and intelligent mechanical devices. For example, White et al. recently prepared LCE fibers by DIW printing and twisting methods. These LCE fibers can rotate, contract, and lift heavy objects when stimulated by heat[143] (Figure 14a). Lu et al. fabricated ultra-fine LCE fibers by MEW printing, and they also fabricated a lattice sensor device that could monitor the temperature in real-time using these fibers. When the ambient temperature field changes, the LCEs mesh in the high-temperature region shrinks and becomes smaller, while the LCEs mesh in the low-temperature region expands and becomes larger[125] (Figure 14b). By using machine vision combined with deep learning model training, high-precision and real-time monitoring of the environmental temperature field is realized. The detection range is from -25°C to 110°C, the average accuracy is 94.79%, and the response time is less than 43 ms. The proposed method is expected to replace traditional thermocouples or fiber-optic distributed sensors.

Soft pneumatic actuators (SPAs) are a kind of mechanical devices that convert gas energy into mechanical energy, and then generate actuation once they are inflated. LCEs have potential applications in fabricated SPAs due to their soft elastic properties. However, conventional method restricts their further development, because it is difficult to fabricate sealed LCE actuators. The emergence of 4D printing technology has, to some extent, solved this problem. With the development of 4D printing technology, this vision will become a reality. Liao et al. have reported a novel method for manufacturing SPAs based on aligned LCEs through improved 3D printing technology.[106] By using a custom-designed 3D printing method equipped with a rotating substrate, the liquid crystal elements can be precisely aligned and programmed to generate the inherent anisotropy with the LCE network. In this way, the LCE-SPA can achieve various actions such as grasping objects (Figure 14c).

Composite materials made from LCEs and other materials have unique advantages in complex applications. With the development of 3D/4D printed multi-materials, new composite materials are constantly emerging. LCEs can undergo swift and reversible shape-change; however, they require a consistent actuation stimulus to preserve their deformed configuration. Shape memory polymers (SMPs) generally have good capacity to maintain their temporary shape, but their actuation ability is not significant. Therefore, it is still a challenge to achieve rapid, reversible, adjustable deformation with good mechanical properties. To address this issue, Qi et al. have fabricated an LCE-SMP composite based on 4D printing.[136] The composite can not only achieve rapid and reversible large deformation, but also can control the shape and maintain a mechanical stiffness of approximately 1 GPa after actuation. They took advantage of the time-dependent distinctions in thermo-mechanical properties between LCE and SMP to regulate the material's high-stiffness structure. Due to the differences in thermal and mechanical properties between LCE and SMP, the composite's structure is fixed by SMP at low temperatures and actuated by LCE at high temperatures. To make this process more observable, the researchers also introduced a thermosensitive dye into the SMP material, giving the SMP different colors at high and low temperatures (Figure 14d).

In addition, through hybrid additive manufacturing, some progress has been made in combining DIW and DLP. Due to the limitation that traditional DIW-printed LCEs cannot be cured immediately, 3D printing of complex LCE structures (such as spatial lattices with rough motion) remains a challenge. Peng et al. came up with a one-step 3D printing method to manufacture an LCE actuator with adaptable stability and a 3D spatial LCE lattice.[108] This process involves a combination of laser-assisted DIW and DLP methods, with the assistance of a removable support structure. This approach provides new insight for applications such as intelligent structures and wearable smart devices.

5.3. Optical Applications. In nature, organisms often exhibit a wide range of colors. Many creatures in nature can change their color in response to danger, when communicating with other species, or when camouflaging in the environment to avoid potential predators. For instance, chameleons can rapidly adjust their skin color to match the background of their environment, butterflies and zebrafish can alter their coloration

https://doi.org/10.1021/cbe.4c00027
Chem Bio Eng. 2024, 1, 488−515

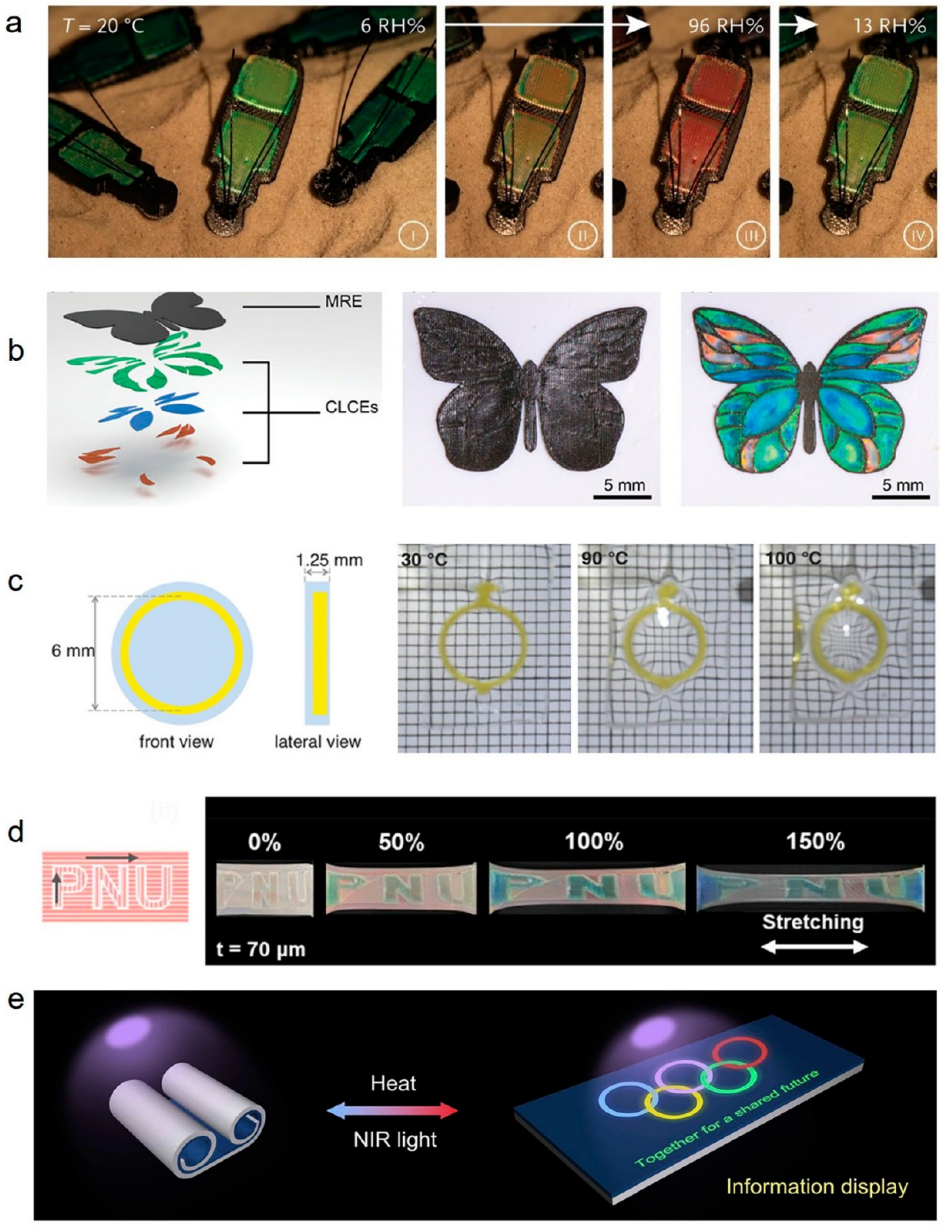

Figure 15. Optical applications of 4D printing of LCEs. (a) 4D printed hygro-sensitive color-changing CLCE actuators.[131] Reproduced with permission. Copyright 2022, John Wiley & Sons, Inc. (b) 4D printed magnetically responsive CLCE actuators capable of simulating the colorful appearance and motion of butterflies.[133] Reproduced with permission. Copyright 2021, John Wiley & Sons, Inc. (c) CLCE-based strain sensor capable of exhibiting intricate color patterns when subjected to stretching.[129] Reproduced with permission. Copyright 2023, John Wiley & Sons, Inc. (d) A light-actuated, deployable LCE information display.[130] Reproduced with permission. Copyright 2023, Elsevier. (e) A lens actuator by incorporating polydimethylsiloxane (PDMS) into a 4D printed LCE aperture.[99] Reproduced with permission. Copyright 2018, John Wiley & Sons, Inc.

in response to varying light conditions, and beetles can change color according to changes in ambient humidity. These interesting natural phenomena have inspired scientists to design and prepare a series of intelligent LCE soft actuators with color-changing functions, and the research has greatly promoted the development of LCEs in the fields of biosensors, visual detection/display and camouflage. At present, 4D printed color-changing LCE soft actuators mainly include three categories: color-changing LCE soft actuators based on cholesteric liquid crystals, color-changing LCE soft actuators doped with inorganic color-changing materials and color-changing LCE soft actuators integrated with other materials.

The principle of the color-changing actuator based on cholesteric liquid crystals is that the LC molecules self-assemble into a layered structure, the molecules in the layer are parallel to each other, and the molecules between the two adjacent layers rotate at a certain angle to form a periodic spiral structure. It can not only selectively reflect circularly polarized light with the same spiral direction as itself, but also exhibit a sensitive response to external stimuli, which allows for dynamic control of its structural color. Although the research of biomimetic color-changing actuators based on cholesteric liquid crystal elastomers (CLCEs) has made some progress,[132,164,165] there is little research on 4D printing of CLCE color-changing actuators.

https://doi.org/10.1021/cbe.4c00027
Chem Bio Eng. 2024, 1, 488−515

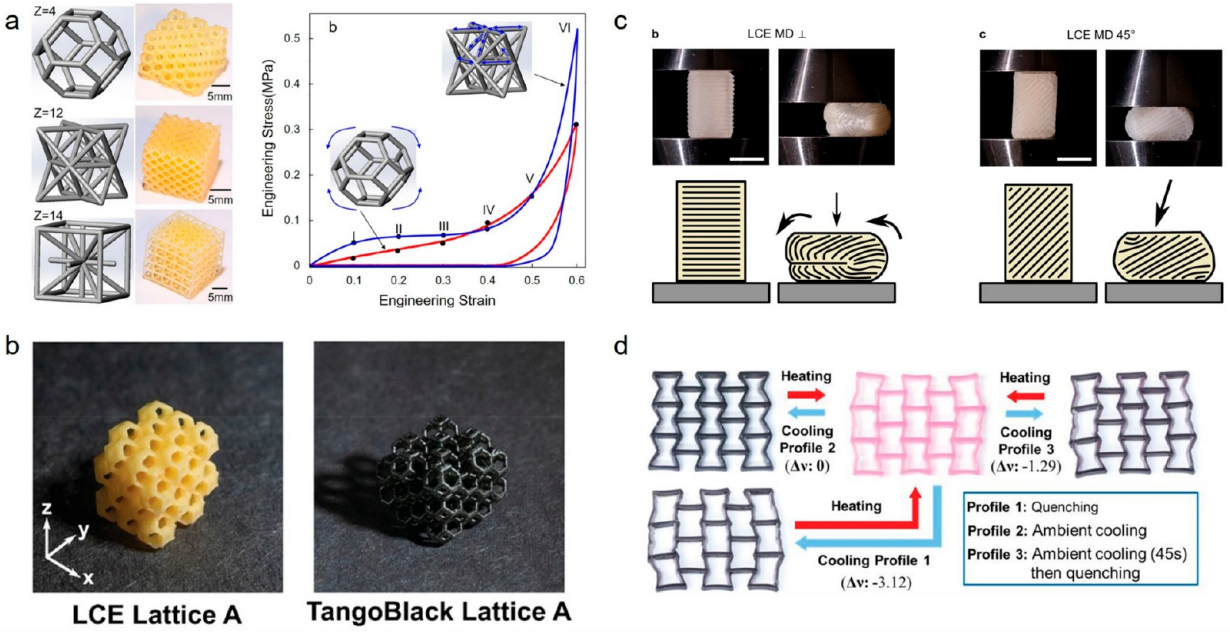

Figure 16. Applications of LCE lattice structures and dissipators. (a) LCE foam cells exhibiting energy dissipation performance.[171] Reproduced with permission. Copyright 2021, American Chemical Society. (b) Complex LCE lattice devices with high resolution.[145] Reproduced with permission. Copyright 2020, John Wiley & Sons, Inc. (c) LCE energy dissipator with a lattice structure fabricated by DIW.[134] Reproduced with permission. Copyright 2021, Springer Nature. (d) Stent-assisted LCE lattice structure showing regular actuation when heated.[136] Reproduced with permission. Copyright 2022, John Wiley & Sons, Inc.

Recently, Debije et al. have fabricated a 4D printed hygro-sensitive color-changing CLCE actuator.[131] They incorporated hygroscopic ammonium groups into CLCEs for 4D printing. After the printed materials are treated with acid and protonated, CLCEs containing hygroscopic ammonium groups are obtained. When the external humidity changes, the CLCE actuators will achieve reversible "on" and "off" actuation due to the different water absorption rates of the hygroscopic ammonium groups in the inner and outer layers. Simultaneously, CLCEs can undergo reversible color changes due to the changes in refractive index caused by water absorption (Figure 15a). The actuator is expected to find use in future intelligent 4D structural coloring devices. Furthermore, they investigated the optical characteristics and actuation performances of CLCE actuators incorporated with azobenzene.[138] Bi et al. fabricated a magnetically responsive CLCE actuator through DIW printing.[133] They have fabricated a bionic butterfly actuator, in which the CLCE layer contributes angle-dependent rainbow colors, while the magnetic responsible elastomer (MRE) layer imparts actuation performance to the bionic robot (Figure 15b). In addition, Choi et al. have printed a ropy CLC ink and subsequently photopolymerized the printed pattern to fabricate a CLCE actuator.[129] They used the anisotropic force-induced chromatism to fabricate a unique CLCE-based strain sensor that is capable of exhibiting intricate color patterns when subjected to stretching, demonstrating significant potential for applications in encryption, anti-counterfeiting, and structural health monitoring (Figure 15c).

Incorporating inorganic photoresponsive materials into LCEs to prepare LCE-based optical devices is also an emerging trend in future developments. The emerging perovskite-polymer composites possess the combined properties of high luminescence and arbitrary deformation, which is of great significance for the next generation of flexible wearable optical devices. Recently, Xiao et al. achieved a development by covalently bonding polymerizable perovskite quantum dots (PQDs) to a silanized polymer surface at the organic-inorganic interface.[130] They subsequently combined PQDs with a 4D-printed deformable LCE using DIW printing to fabricate a light-actuated, deployable information display LCE actuator (Figure 15d).

The integration of 4D-printed LCE with other materials into adaptive optics is also a future development trend. Lopez et al. prepared a lens actuator by incorporating polydimethylsiloxane (PDMS) into a 4D printed LCE aperture.[99] By reversibly controlling the temperature, the LCE aperture can be reversibly actuated to change the focusing characteristics of the lens. This actuator has potential applications in adaptive optics (Figure 15e).

5.4. LCE Lattice Structures and Dissipators. The lattice structure is known for its low density and good mechanical properties.[166] It typically utilizes periodic and porous basic element arrangements to form a geometric pattern with regularity and stability. Lattice structures have wide applications in various fields, including materials science, architecture, and aerospace engineering, because of their ability to reduce mass, increase stiffness and impact resistance, while maintaining good fatigue and deformation recovery properties. Lattice structures were progressively developed in many studies during the 20th century. However, the rapid development of lattice structures can be attributed to the breakthrough of 3D printing technology in the early 2000s. This technology makes it possible to design and manufacture complex geometric shapes and topologies. With the development of 3D printing technology, more and more research and applications are focused on lattice structures, enabling a rapid growth of this field. LCE has both the anisotropy of liquid crystal and the entropic elasticity of rubber due to its light crosslinked structure. This characteristic feature makes LCEs possess a large energy dissipation capacity.[167−170] In vivo, numerous load-bearing biological tissues display

https://doi.org/10.1021/cbe.4c00027
Chem Bio Eng. 2024, 1, 488−515

intricate layered structures similar to lattice structures. Consequently, the advancement of 4D-printed LCE with lattice structures is becoming increasingly crucial. Recently, some research has achieved significant breakthroughs in this area.

DLP 3D printing possesses a significant advantage in fabricating lattice structures with specific micro and macro architectures because of its high resolution and the ability to fabricate layered complex structures. Luo et al. fabricated LCE foam cells using DLP[171] (Figure 16a). They investigated the influence of the geometry of the cell and the mechanical properties of the base material on the energy dissipation of the soft polymer foam. The results show that the energy dissipation ratio of LCE lattice structure is 3.9 times higher than that of non-LCE lattice structure. While temperature has minimal influence on the energy dissipation performance of the LCE lattice. Traugutt et al. first prepared a new light-curable mercaptoacrylate LC ink to 3D print complex LCE lattice devices with high resolution[145] (Figure 16b). Compared to commercially available LCEs like TangoBlack, this LCE exhibits remarkable performance, and under dynamic conditions, the energy absorbed by the LCE lattice is 5-27 times that of the TangoBlack lattice.

Shaha et al. prepared 4D-printed LCEs to mimic intervertebral discs. The LCEs can match the anisotropic mechanical behaviors of the discs. In vivo animal experiments have proved that LCEs exhibit good biocompatibility when implanted subcutaneously. In another study, polythene monomer copolymerization was incorporated into the system, and the impact of crystallization properties on the stability of the LCE disc was also examined.[167] Cai et al. used DIW to 3D print an LCE actuator with gradient characteristics, capable of achieving a maximum actuation strain of 20%. Mistry et al. utilized layer-by-layer photocuring DIW to fabricate an LCE energy dissipator with a lattice structure[134] (Figure 16c). They discovered that the excellent soft elasticity of the single-domain lattice structure imparted superior energy dissipation properties to the LCEs, surpassing traditional isotropic elastomers. The single domain soft elastic LCE could dissipate 45% strain energy, which is expected to be applied in the field of energy shock absorber. Recently, Qi and co-workers prepared SMP and LCE composite lattices through DLP, which possess good load-bearing capacity[136] (Figure 16d). They also integrated DLP with DIW technology to 3D print a stent-assisted LCE lattice structure, exhibiting regular actuation upon heating.[108]

6. PERSPECTIVE AND OUTLOOK

LCEs are composed of anisotropic LC units and elastic polymer networks, which show rapid and large reversible deformations under external stimuli, thus exhibiting extensive application prospects in various fields, including artificial muscles, soft robots and bionic intelligent devices. In nature, based on their complex structure-function interrelationships, organisms are able to make precise and intricate movements in response to environmental stimuli. This phenomenon has inspired scientists to develop LCE actuators with hierarchical structures and intricate deformations. Nevertheless, using traditional methods to manufacture these LCE actuators with complex structures has some limitations. 4D printing refers to the additive manufacturing of stimulus-responsive materials, enabling 3D structures to vary between predetermined shapes. This approach not only simplifies the manufacturing process of traditional LCE actuators, but also allows for the preparation of complex LCE structures with multi-level mesogen orientation, which provides great flexibility for researchers to design LCE actuators with sophisticated structures. Nevertheless, there are still some challenges that 4D-printed LCEs have to face.

(1) For 3D and 4D printing of LCEs, a primary problem that needs to be addressed is the printing technologies (printing method, ink formulation, orientation method, cross-linking method, printing structure, etc.) that need further improvement. Among these various printing methods, DIW is the most widely used printing technology for the preparation of LCE actuators. However, at present, the types of LC inks suitable for DIW printing are still relatively few. Inks are mainly LC oligomers obtained by the Michael addition reaction of amine-acrylate or thiol−acrylate, and the shape of the orientation LCE structure needs to be fixed by additional photo-cross-linking after printing. Although DIW printing has advantages in fabricating large-size 1D and 2D LCEs, its resolution is low and it lacks preponderance in fabricating LCEs with 3D structures. MEW printing has advantages in the preparation of ultrafine LCE fibers but also has the problem of high equipment requirements. TPP-DLW and DLP printing are still in their infancy. Both printing technologies require further expansion of the range of inks that can be printed. However, due to the high resolution of TPP-DLW and DLP, as well as the significant advantages in preparing LCEs with 3D lattice structures, these technologies represent a crucial research direction for future development. In addition, the new methods of 3D printing are also the future development directions for LCEs, such as the multi-material spiral extrusion printing[172] and so on.

(2) Reconfigurable 4D printed LCEs are the future research direction. LCE actuators are usually covalently cross-linked networks and cannot be changed once they are formed, which prevents the materials from being recycled and also limits the deformation diversity. Dynamic bond is a kind of special chemical bond, including both covalent dynamic bond and non-covalent dynamic bond, which can be broken and regenerated under external stimuli. The introduction of dynamic bonds into LCEs provides them with a variety of features, such as enhanced mechanical performance, self-healing ability and reprogrammable properties, thus increasingly attracting research interests.[173] Nevertheless, the research of LCEs with dynamic bonds is still in the early stage, so it is of great significance to develop new dynamic LCEs suitable for 4D printing.

(3) The range of applications for 4D-printed LCEs needs further broadening. At present LCEs have achieved some practical applications in industrial production. However, as a kind of intelligent stimuli-responsive soft material, LCE is expected to be widely used in emerging fields such as human-computer interaction, intelligent robots, wearable devices, and health monitoring. Several existing challenges have hindered the development of LCEs. For thermally activated LCEs, the high driving temperature limits their applications. Additionally, for most light-driven LCEs, the reliance on UV light is a concern due to its potential harm to the human body. Hence, scientists need to develop LCEs that can respond to visible light, and even to near-infrared light. Furthermore, the development of emerging magnetically and electrically responsive LCEs is also a future trend to endow LCEs

https://doi.org/10.1021/cbe.4c00027
Chem Bio Eng. 2024, 1, 488−515

with more remote response capabilities. In addition, 4D-printed LCEs need further broaden their actuation environment to meet different requirements. Such as extremely low temperatures,[174] chemical solvents,[175] and so on. In addition, 4D printed micro-actuators need to be further developed.[147]

(4) Additionally, with the progress of material science, the development of composite actuators integrating LCEs with hydrogels, shape memory polymers (SMPs), and other materials holds practical significance. This approach leads to new LCE-based composite materials responsive to multiple stimuli, thereby enriching their practical applications.

In conclusion, although significant advancements have been made in 4D printed LCEs, important scientific and practical challenges remain in fabricating large-scale, high-resolution, and multi-stimuli-responsive LCEs. It is believed that with the development of 4D printing technologies, the continuous evolution of AI modeling technology, and the advancements in materials science, more and more progress can be made in the promising research field of 4D printed shape-morphing LCEs.

AUTHOR INFORMATION

Corresponding Authors

Xili Lu − *State Key Laboratory of Polymer Materials Engineering, Polymer Research Institute, Sichuan University, Chengdu 610065, China;* orcid.org/0000-0003-3705-3694; Email: xililu@scu.edu.cn

Jianshe Hu − *Center for Molecular Science and Engineering, College of Science, Northeastern University, Shenyang 110819, China;* orcid.org/0000-0003-0624-0788; Email: hujs@mail.neu.edu.cn

Hesheng Xia − *State Key Laboratory of Polymer Materials Engineering, Polymer Research Institute, Sichuan University, Chengdu 610065, China;* orcid.org/0000-0001-8087-7272; Email: xiahs@scu.edu.cn

Yue Zhao − *Département de chimie, Université de Sherbrooke, Sherbrooke, Québec J1K 2R1, Canada;* orcid.org/0000-0001-5544-5697; Email: yue.zhao@usherbrooke.ca

Authors

Tongzhi Zang − *State Key Laboratory of Polymer Materials Engineering, Polymer Research Institute, Sichuan University, Chengdu 610065, China; Center for Molecular Science and Engineering, College of Science, Northeastern University, Shenyang 110819, China*

Shuang Fu − *State Key Laboratory of Polymer Materials Engineering, Polymer Research Institute, Sichuan University, Chengdu 610065, China*

Junpeng Cheng − *State Key Laboratory of Polymer Materials Engineering, Polymer Research Institute, Sichuan University, Chengdu 610065, China*

Chun Zhang − *State Key Laboratory of Polymer Materials Engineering, Polymer Research Institute, Sichuan University, Chengdu 610065, China*

Complete contact information is available at: https://pubs.acs.org/10.1021/cbe.4c00027

Notes

The authors declare no competing financial interest.

ACKNOWLEDGMENTS

This work was financially supported by the National Natural Science Foundation of China (No. 52103145) and the Science & Technology Department of Sichuan Province (No. 2022YFH0091).

REFERENCES

(1) Ngo, T. D.; Kashani, A.; Imbalzano, G.; Nguyen, K. T. Q.; Hui, D. Additive manufacturing (3D printing): A review of materials, methods, applications and challenges. *Compos. B. Eng.* **2018**, *143*, 172−196.

(2) Tibbits, S. 4D Printing: Multi-Material Shape Change. *Archit. Des.* **2014**, *84* (1), 116−121.

(3) Momeni, F.; M.Mehdi Hassani.N, S.; Liu, X.; Ni, J. A review of 4D printing. *Mater. Des.* **2017**, *122*, 42−79.

(4) Sydney Gladman, A.; Matsumoto, E. A.; Nuzzo, R. G.; Mahadevan, L.; Lewis, J. A. Biomimetic 4D printing. *Nat. Mater.* **2016**, *15* (4), 413−418.

(5) Tang, T.; Alfarhan, S.; Jin, K.; Li, X. 4D Printing of Seed Capsule-Inspired Hygro-Responsive Structures via Liquid Crystal Templating-Assisted Vat Photopolymerization. *Adv. Funct. Mater.* **2023**, *33* (5), No. 2211602.

(6) Yang, H.; Leow, W. R.; Wang, T.; Wang, J.; Yu, J.; He, K.; Qi, D.; Wan, C.; Chen, X. 3D Printed Photoresponsive Devices Based on Shape Memory Composites. *Adv. Mater.* **2017**, *29* (33), No. 1701627.

(7) Ding, Z.; Yuan, C.; Peng, X.; Wang, T.; Qi, H. J.; Dunn, M. L. Direct 4D printing via active composite materials. *Sci. Adv.* **2017**, *3* (4), No. e1602890.

(8) Kim, Y.; Yuk, H.; Zhao, R.; Chester, S. A.; Zhao, X. Printing ferromagnetic domains for untethered fast-transforming soft materials. *Nature.* **2018**, *558* (7709), 274−279.

(9) Nadgorny, M.; Xiao, Z.; Chen, C.; Connal, L. A. Three-Dimensional Printing of pH-Responsive and Functional Polymers on an Affordable Desktop Printer. *ACS Appl. Mater. Interfaces.* **2016**, *8* (42), 28946−28954.

(10) Ge, Q.; Sakhaei, A. H.; Lee, H.; Dunn, C. K.; Fang, N. X.; Dunn, M. L. Multimaterial 4D Printing with Tailorable Shape Memory Polymers. *Sci. Rep.* **2016**, *6* (1), 31110.

(11) Miao, S.; Zhu, W.; Castro, N. J.; Nowicki, M.; Zhou, X.; Cui, H.; Fisher, J. P.; Zhang, L. G. 4D printing smart biomedical scaffolds with novel soybean oil epoxidized acrylate. *Sci. Rep.* **2016**, *6* (1), 27226.

(12) Kokkinis, D.; Schaffner, M.; Studart, A. R. Multimaterial magnetically assisted 3D printing of composite materials. *Nat. Commun.* **2015**, *6* (1), 8643.

(13) Bakarich, S. E.; Gorkin, R., 3rd; in het Panhuis, M.; Spinks, G. M. 4D Printing with Mechanically Robust, Thermally Actuating Hydrogels. *Macromol. Rapid Commun.* **2015**, *36* (12), 1211−7.

(14) Zhang, W.; Zhang, F.; Lan, X.; Leng, J.; Wu, A. S.; Bryson, T. M.; Cotton, C.; Gu, B.; Sun, B.; Chou, T.-W. Shape memory behavior and recovery force of 4D printed textile functional composites. *Compos Sci. Technol.* **2018**, *160*, 224−230.

(15) Khoshnevis, B. Automated construction by contour crafting—related robotics and information technologies. *Autom. Constr.* **2004**, *13* (1), 5−19.

(16) Kuang, X.; Roach, D. J.; Wu, J.; Hamel, C. M.; Ding, Z.; Wang, T.; Dunn, M. L.; Qi, H. J. Advances in 4D Printing: Materials and Applications. *Adv. Funct. Mater.* **2019**, *29* (2), No. 1805290.

(17) Meng, H.; Li, G. A review of stimuli-responsive shape memory polymer composites. *Polymer.* **2013**, *54* (9), 2199−2221.

(18) Chen, M.; Gao, M.; Bai, L.; Zheng, H.; Qi, H. J.; Zhou, K. Recent Advances in 4D Printing of Liquid Crystal Elastomers. *Adv. Mater.* **2023**, *35* (23), No. 2209566.

(19) Ohm, C.; Brehmer, M.; Zentel, R. Liquid Crystalline Elastomers as Actuators and Sensors. *Adv. Mater.* **2010**, *22* (31), 3366−3387.

(20) Jin, B.; Yang, S. Programming Liquid Crystalline Elastomer Networks with Dynamic Covalent Bonds. *Adv. Funct. Mater.* **2023**, *33* (45), No. 2304769.

(21) Kularatne, R. S.; Kim, H.; Boothby, J. M.; Ware, T. H. Liquid crystal elastomer actuators: Synthesis, alignment, and applications. *J. Polym. Sci. B Polym. Phys.* **2017**, *55* (5), 395−411.
(22) Guan, Z.; Wang, L.; Bae, J. Advances in 4D printing of liquid crystalline elastomers: materials, techniques, and applications. *Mater. Horiz.* **2022**, *9* (7), 1825−1849.
(23) Wang, Z.; Guo, Y.; Cai, S.; Yang, J. Three-Dimensional Printing of Liquid Crystal Elastomers and Their Applications. *ACS Appl. Polym. Mater.* **2022**, *4* (5), 3153−3168.
(24) del Pozo, M.; Sol, J. A. H. P.; Schenning, A. P. H. J.; Debije, M. G. 4D Printing of Liquid Crystals: What's Right for Me? *Adv. Mater.* **2022**, *34* (3), No. 2104390.
(25) Xiao, Y.; Wu, J.; Zhang, Y. Recent advances in the design, fabrication, actuation mechanisms and applications of liquid crystal elastomers. *Soft Sci.* **2023**, *3* (2), 11.
(26) Wan, X.; Luo, L.; Liu, Y.; Leng, J. Direct Ink Writing Based 4D Printing of Materials and Their Applications. *Adv. Sci.* **2020**, *7* (16), No. 2001000.
(27) Yang, R.; Wang, Y.; Yao, H.; Li, Y.; Chen, L.; Zhao, Y.; Wang, Y.-Z. Dynamic Shape Change of Liquid Crystal Polymer Based on An Order-Order Phase Transition. *Angew. Chem. Int. Ed.* **2024**, *63* (9), No. e202314859.
(28) Finkelmann, H.; Kock, H.-J.; Rehage, G. Investigations on liquid crystalline polysiloxanes 3. Liquid crystalline elastomers — a new type of liquid crystalline material. *Makromol. Chem., Rapid Commun.* **1981**, *2* (4), 317−322.
(29) Thomsen, D. L.; Keller, P.; Naciri, J.; Pink, R.; Jeon, H.; Shenoy, D.; Ratna, B. R. Liquid Crystal Elastomers with Mechanical Properties of a Muscle. *Macromolecules* **2001**, *34* (17), 5868−5875.
(30) White, T. J.; Broer, D. J. Programmable and adaptive mechanics with liquid crystal polymer networks and elastomers. *Nat. Mater.* **2015**, *14* (11), 1087−1098.
(31) Yang, Y.; Terentjev, E. M.; Zhang, Y.; Chen, Q.; Zhao, Y.; Wei, Y.; Ji, Y. Reprocessable Thermoset Soft Actuators. *Angew. Chem. Int. Ed.* **2019**, *58* (48), 17474−17479.
(32) Hu, Z.; Li, Y.; Lv, J.-a. Phototunable self-oscillating system driven by a self-winding fiber actuator. *Nat. Commun.* **2021**, *12* (1), 3211.
(33) Liu, L.; Liu, M.-H.; Deng, L.-L.; Lin, B.-P.; Yang, H. Near-Infrared Chromophore Functionalized Soft Actuator with Ultrafast Photoresponsive Speed and Superior Mechanical Property. *J. Am. Chem. Soc.* **2017**, *139* (33), 11333−11336.
(34) Wani, O. M.; Zeng, H.; Priimagi, A. A light-driven artificial flytrap. *Nat. Commun.* **2017**, *8* (1), 15546.
(35) Kotikian, A.; McMahan, C.; Davidson, E. C.; Muhammad, J. M.; Weeks, R. D.; Daraio, C.; Lewis, J. A. Untethered soft robotic matter with passive control of shape morphing and propulsion. *Sci. Robot.* **2019**, *4* (33), No. eaax7044.
(36) Gelebart, A. H.; Jan Mulder, D.; Varga, M.; Konya, A.; Vantomme, G.; Meijer, E. W.; Selinger, R. L. B.; Broer, D. J. Making waves in a photoactive polymer film. *Nature.* **2017**, *546* (7660), 632−636.
(37) Camacho-Lopez, M.; Finkelmann, H.; Palffy-Muhoray, P.; Shelley, M. Fast liquid-crystal elastomer swims into the dark. *Nat. Mater.* **2004**, *3* (5), 307−310.
(38) Wang, C.; Sim, K.; Chen, J.; Kim, H.; Rao, Z.; Li, Y.; Chen, W.; Song, J.; Verduzco, R.; Yu, C. Soft Ultrathin Electronics Innervated Adaptive Fully Soft Robots. *Adv. Mater.* **2018**, *30* (13), No. 1706695.
(39) Xiao, Y.-Y.; Jiang, Z.-C.; Tong, X.; Zhao, Y. Biomimetic Locomotion of Electrically Powered "Janus" Soft Robots Using a Liquid Crystal Polymer. *Adv. Mater.* **2019**, *31* (36), No. 1903452.
(40) Martella, D.; Nocentini, S.; Nuzhdin, D.; Parmeggiani, C.; Wiersma, D. S. Photonic Microhand with Autonomous Action. *Adv. Mater.* **2017**, *29* (42), No. 1704047.
(41) Li, C.; Liu, Y.; Huang, X.; Jiang, H. Direct Sun-Driven Artificial Heliotropism for Solar Energy Harvesting Based on a Photo-Thermomechanical Liquid-Crystal Elastomer Nanocomposite. *Adv. Funct. Mater.* **2012**, *22* (24), 5166−5174.
(42) Zhang, C.; Fei, G.; Lu, X.; Xia, H.; Zhao, Y. Liquid Crystal Elastomer Artificial Tendrils with Asymmetric Core−Sheath Structure Showing Evolutionary Biomimetic Locomotion. *Adv. Mater.* **2024**, *36*, No. 2307210.
(43) Schuhladen, S.; Preller, F.; Rix, R.; Petsch, S.; Zentel, R.; Zappe, H. Iris-Like Tunable Aperture Employing Liquid-Crystal Elastomers. *Adv. Mater.* **2014**, *26* (42), 7247−7251.
(44) Buguin, A.; Li, M.-H.; Silberzan, P.; Ladoux, B.; Keller, P. Micro-Actuators: When Artificial Muscles Made of Nematic Liquid Crystal Elastomers Meet Soft Lithography. *J. Am. Chem. Soc.* **2006**, *128* (4), 1088−1089.
(45) Li, M. H.; Keller, P.; Yang, J.; Albouy, P. A. An Artificial Muscle with Lamellar Structure Based on a Nematic Triblock Copolymer. *Adv. Mater.* **2004**, *16* (21), 1922−1925.
(46) Shenoy, D. K.; Thomsen, D. L., III; Srinivasan, A.; Keller, P.; Ratna, B. R. Carbon coated liquid crystal elastomer film for artificial muscle applications. *Sens. Actuator A Phys.* **2002**, *96* (2), 184−188.
(47) Torras, N.; Zinoviev, K. E.; Camargo, C. J.; Campo, E. M.; Campanella, H.; Esteve, J.; Marshall, J. E.; Terentjev, E. M.; Omastová, M.; Krupa, I.; Teplický, P.; Mamojka, B.; Bruns, P.; Roeder, B.; Vallribera, M.; Malet, R.; Zuffanelli, S.; Soler, V.; Roig, J.; Walker, N.; Wenn, D.; Vossen, F.; Crompvoets, F. M. H. Tactile device based on opto-mechanical actuation of liquid crystal elastomers. *Sens. Actuator A Phys.* **2014**, *208*, 104−112.
(48) Wang, Y.; Liao, W.; Sun, J.; Nandi, R.; Yang, Z. Bioinspired Construction of Artificial Cardiac Muscles Based on Liquid Crystal Elastomer Fibers. *Adv. Mater. Technol.* **2022**, *7* (1), No. 2100934.
(49) Lv, J.-a.; Liu, Y.; Wei, J.; Chen, E.; Qin, L.; Yu, Y. Photocontrol of fluid slugs in liquid crystal polymer microactuators. *Nature.* **2016**, *537* (7619), 179−184.
(50) Yuan, C.; Roach, D. J.; Dunn, C. K.; Mu, Q.; Kuang, X.; Yakacki, C. M.; Wang, T. J.; Yu, K.; Qi, H. J. 3D printed reversible shape changing soft actuators assisted by liquid crystal elastomers. *Soft Matter.* **2017**, *13* (33), 5558−5568.
(51) Xia, Y.; Cedillo-Servin, G.; Kamien, R. D.; Yang, S. Guided Folding of Nematic Liquid Crystal Elastomer Sheets into 3D via Patterned 1D Microchannels. *Adv. Mater.* **2016**, *28* (43), 9637−9643.
(52) Ware, T. H.; McConney, M. E.; Wie, J. J.; Tondiglia, V. P.; White, T. J. Voxelated liquid crystal elastomers. *Science.* **2015**, *347* (6225), 982−984.
(53) Guin, T.; Settle, M. J.; Kowalski, B. A.; Auguste, A. D.; Beblo, R. V.; Reich, G. W.; White, T. J. Layered liquid crystal elastomer actuators. *Nat. Commun.* **2018**, *9* (1), 2531.
(54) Kim, H.; Boothby, J. M.; Ramachandran, S.; Lee, C. D.; Ware, T. H. Tough, Shape-Changing Materials: Crystallized Liquid Crystal Elastomers. *Macromolecules* **2017**, *50* (11), 4267−4275.
(55) Shahsavan, H.; Salili, S. M.; Jákli, A.; Zhao, B. Thermally Active Liquid Crystal Network Gripper Mimicking the Self-Peeling of Gecko Toe Pads. *Adv. Mater.* **2017**, *29* (3), No. 1604021.
(56) Zhang, C.; Lu, X.; Fei, G.; Wang, Z.; Xia, H.; Zhao, Y. 4D Printing of a Liquid Crystal Elastomer with a Controllable Orientation Gradient. *ACS Appl. Mater. Interfaces.* **2019**, *11* (47), 44774−44782.
(57) Lu, X.; Zhang, H.; Fei, G.; Yu, B.; Tong, X.; Xia, H.; Zhao, Y. Liquid-Crystalline Dynamic Networks Doped with Gold Nanorods Showing Enhanced Photocontrol of Actuation. *Adv. Mater.* **2018**, *30* (14), No. 1706597.
(58) Zeng, H.; Wani, O. M.; Wasylczyk, P.; Kaczmarek, R.; Priimagi, A. Self-Regulating Iris Based on Light-Actuated Liquid Crystal Elastomer. *Adv. Mater.* **2017**, *29* (30), No. 1701814.
(59) Shahsavan, H.; Aghakhani, A.; Zeng, H.; Guo, Y.; Davidson, Z. S.; Priimagi, A.; Sitti, M. Bioinspired underwater locomotion of light-driven liquid crystal gels. *Proc. Natl. Acad. Sci. U. S. A.* **2020**, *117* (10), 5125−5133.
(60) Hauser, A. W.; Liu, D.; Bryson, K. C.; Hayward, R. C.; Broer, D. J. Reconfiguring Nanocomposite Liquid Crystal Polymer Films with Visible Light. *Macromolecules* **2016**, *49* (5), 1575−1581.
(61) Yang, Y.; Pei, Z.; Li, Z.; Wei, Y.; Ji, Y. Making and Remaking Dynamic 3D Structures by Shining Light on Flat Liquid Crystalline Vitrimer Films without a Mold. *J. Am. Chem. Soc.* **2016**, *138* (7), 2118−2121.

(62) Ahir, S. V.; Terentjev, E. M. Photomechanical actuation in polymer−nanotube composites. *Nat. Mater.* **2005**, *4* (6), 491−495.
(63) Marshall, J. E.; Ji, Y.; Torras, N.; Zinoviev, K.; Terentjev, E. M. Carbon-nanotube sensitized nematic elastomer composites for IR-visible photo-actuation. *Soft Matter.* **2012**, *8* (5), 1570−1574.
(64) Wu, Y.; Zhang, S.; Yang, Y.; Li, Z.; Wei, Y.; Ji, Y. Locally controllable magnetic soft actuators with reprogrammable contraction-derived motions. *Sci. Adv.* **2022**, *8* (25), No. eabo6021.
(65) Haberl, J. M.; Sánchez-Ferrer, A.; Mihut, A. M.; Dietsch, H.; Hirt, A. M.; Mezzenga, R. Liquid-Crystalline Elastomer-Nanoparticle Hybrids with Reversible Switch of Magnetic Memory. *Adv. Mater.* **2013**, *25* (12), 1787−1791.
(66) Winkler, M.; Kaiser, A.; Krause, S.; Finkelmann, H.; Schmidt, A. M. Liquid Crystal Elastomers with Magnetic Actuation. *Macromol. Symp.* **2010**, *291-292* (1), 186−192.
(67) Wang, H.; Yang, Y.; Zhang, M.; Wang, Q.; Xia, K.; Yin, Z.; Wei, Y.; Ji, Y.; Zhang, Y. Electricity-Triggered Self-Healing of Conductive and Thermostable Vitrimer Enabled by Paving Aligned Carbon Nanotubes. *ACS Appl. Mater. Interfaces.* **2020**, *12* (12), 14315−14322.
(68) Finkelmann, H.; Shahinpoor, M. Electrically controllable liquid crystal elastomer-graphite composite artifical muscles. *Proc. SPIE* **2002**, 459−464.
(69) Courty, S.; Mine, J.; Tajbakhsh, A. R.; Terentjev, E. M. Nematic elastomers with aligned carbon nanotubes: New electromechanical actuators. *Europhys. Lett.* **2003**, *64* (5), 654.
(70) Lu, X.; Guo, S.; Tong, X.; Xia, H.; Zhao, Y. Tunable Photocontrolled Motions Using Stored Strain Energy in Malleable Azobenzene Liquid Crystalline Polymer Actuators. *Adv. Mater.* **2017**, *29* (28), No. 1606467.
(71) Lu, X.; Ambulo, C. P.; Wang, S.; Rivera-Tarazona, L. K.; Kim, H.; Searles, K.; Ware, T. H. 4D-Printing of Photoswitchable Actuators. *Angew. Chem. Int. Ed.* **2021**, *60* (10), 5536−5543.
(72) Aßhoff, S. J.; Lancia, F.; Iamsaard, S.; Matt, B.; Kudernac, T.; Fletcher, S. P.; Katsonis, N. High-Power Actuation from Molecular Photoswitches in Enantiomerically Paired Soft Springs. *Angew. Chem. Int. Ed.* **2017**, *56* (12), 3261−3265.
(73) Feng, W.; Broer, D. J.; Liu, D. Oscillating Chiral-Nematic Fingerprints Wipe Away Dust. *Adv. Mater.* **2018**, *30* (11), No. 1704970.
(74) Davidson, Z. S.; Shahsavan, H.; Aghakhani, A.; Guo, Y.; Hines, L.; Xia, Y.; Yang, S.; Sitti, M. Monolithic shape-programmable dielectric liquid crystal elastomer actuators. *Sci. Adv.* **2019**, *5* (11), No. eaay0855.
(75) Lehmann, W.; Skupin, H.; Tolksdorf, C.; Gebhard, E.; Zentel, R.; Krüger, P.; Lösche, M.; Kremer, F. Giant lateral electrostriction in ferroelectric liquid-crystalline elastomers. *Nature.* **2001**, *410* (6827), 447−450.
(76) Ringsdorf, H.; Zentel, R. Liquid crystalline side chain polymers and their behaviour in the electric field. *Makromol. Chem.* **1982**, *183* (5), 1245−1256.
(77) Guo, Y.; Shahsavan, H.; Sitti, M. 3D Microstructures of Liquid Crystal Networks with Programmed Voxelated Director Fields. *Adv. Mater.* **2020**, *32* (38), No. 2002753.
(78) Guo, S.; De Wolf, S.; Sitti, M.; Serre, C.; Tan, S. C. Hygroscopic Materials. *Adv. Mater.* **2024**, *36* (12), No. 2311445.
(79) Ryabchun, A.; Lancia, F.; Nguindjel, A.-D.; Katsonis, N. Humidity-responsive actuators from integrating liquid crystal networks in an orienting scaffold. *Soft Matter.* **2017**, *13* (44), 8070−8075.
(80) de Haan, L. T.; Verjans, J. M. N.; Broer, D. J.; Bastiaansen, C. W. M.; Schenning, A. P. H. J. Humidity-Responsive Liquid Crystalline Polymer Actuators with an Asymmetry in the Molecular Trigger That Bend, Fold, and Curl. *J. Am. Chem. Soc.* **2014**, *136* (30), 10585−10588.
(81) Herbert, K. M.; Fowler, H. E.; McCracken, J. M.; Schlafmann, K. R.; Koch, J. A.; White, T. J. Synthesis and alignment of liquid crystalline elastomers. *Nat. Rev. Mater.* **2022**, *7* (1), 23−38.
(82) Schadt, M. Liquid crystal displays, LC-materials and LPP photo-alignment. *Mol. Cryst. Liq. Cryst.* **2017**, *647* (1), 253−268.
(83) Murray, B. S.; Pelcovits, R. A.; Rosenblatt, C. Creating arbitrary arrays of two-dimensional topological defects. *Phys. Rev.* **2014**, *90* (5), No. 052501.
(84) Kumar, S.; Kim, J.-H.; Shi, Y. What Aligns Liquid Crystals on Solid Substrates? The Role of Surface Roughness Anisotropy. *Phys. Rev. Lett.* **2005**, *94* (7), No. 077803.
(85) Wang, Y.; Liu, J.; Yang, S. Multi-functional liquid crystal elastomer composites. *Appl. Phys. Rev.* **2022**, *9* (1), No. 011301.
(86) Wang, W.; Sun, X.; Wu, W.; Peng, H.; Yu, Y. Photoinduced Deformation of Crosslinked Liquid-Crystalline Polymer Film Oriented by a Highly Aligned Carbon Nanotube Sheet. *Angew. Chem. Int. Ed.* **2012**, *51* (19), 4644−4647.
(87) Liu, D.; Bastiaansen, C. W. M.; den Toonder, J. M. J.; Broer, D. J. Photo-Switchable Surface Topologies in Chiral Nematic Coatings. *Angew. Chem. Int. Ed.* **2012**, *51* (4), 892−896.
(88) Ge, S.-J.; Zhao, T.-P.; Wang, M.; Deng, L.-L.; Lin, B.-P.; Zhang, X.-Q.; Sun, Y.; Yang, H.; Chen, E.-Q. A homeotropic main-chain tolane-type liquid crystal elastomer film exhibiting high anisotropic thermal conductivity. *Soft Matter.* **2017**, *13* (32), 5463−5468.
(89) van Oosten, C. L.; Bastiaansen, C. W. M.; Broer, D. J. Printed artificial cilia from liquid-crystal network actuators modularly driven by light. *Nat. Mater.* **2009**, *8* (8), 677−682.
(90) Yu, Y.; Maeda, T.; Mamiya, J.-i.; Ikeda, T. Photomechanical Effects of Ferroelectric Liquid-Crystalline Elastomers Containing Azobenzene Chromophores. *Angew. Chem. Int. Ed.* **2007**, *46* (6), 881−883.
(91) Küpfer, J.; Finkelmann, H. Nematic liquid single crystal elastomers. *Makromol. Chem. Rapid Commun.* **1991**, *12* (12), 717−726.
(92) Ube, T.; Kawasaki, K.; Ikeda, T. Photomobile Liquid-Crystalline Elastomers with Rearrangeable Networks. *Adv. Mater.* **2016**, *28* (37), 8212−8217.
(93) Yakacki, C. M.; Saed, M.; Nair, D. P.; Gong, T.; Reed, S. M.; Bowman, C. N. Tailorable and programmable liquid-crystalline elastomers using a two-stage thiol−acrylate reaction. *RSC Adv.* **2015**, *5* (25), 18997−19001.
(94) Ambulo, C. P.; Burroughs, J. J.; Boothby, J. M.; Kim, H.; Shankar, M. R.; Ware, T. H. Four-dimensional Printing of Liquid Crystal Elastomers. *ACS Appl. Mater. Interfaces.* **2017**, *9* (42), 37332−37339.
(95) Kotikian, A.; Truby, R. L.; Boley, J. W.; White, T. J.; Lewis, J. A. 3D Printing of Liquid Crystal Elastomeric Actuators with Spatially Programed Nematic Order. *Adv. Mater.* **2018**, *30* (10), No. 1706164.
(96) Kloxin, C. J.; Bowman, C. N. Covalent adaptable networks: smart, reconfigurable and responsive network systems. *Chem. Soc. Rev.* **2013**, *42* (17), 7161−7173.
(97) Pei, Z.; Yang, Y.; Chen, Q.; Terentjev, E. M.; Wei, Y.; Ji, Y. Mouldable liquid-crystalline elastomer actuators with exchangeable covalent bonds. *Nat. Mater.* **2014**, *13* (1), 36−41.
(98) Fan, Y.; Liu, T.; Li, Y.; Miao, X.; Chen, B.; Ding, J.; Dong, Z.; Rios, O.; Bao, B.; Lin, Q.; Zhu, L. One-Step Manufacturing of Supramolecular Liquid-Crystal Elastomers by Stress-Induced Alignment and Hydrogen Bond Exchange. *Angew. Chem. Int. Ed.* **2023**, *62* (37), No. e202308793.
(99) López-Valdeolivas, M.; Liu, D.; Broer, D. J.; Sánchez-Somolinos, C. 4D Printed Actuators with Soft-Robotic Functions. *Macromol. Rapid Commun.* **2018**, *39* (5), No. 1700710.
(100) Lugger, S. J. D.; Ceamanos, L.; Mulder, D. J.; Sánchez-Somolinos, C.; Schenning, A. P. H. J. 4D Printing of Supramolecular Liquid Crystal Elastomer Actuators Fueled by Light. *Adv. Mater. Technol.* **2023**, *8* (5), No. 2201472.
(101) Ambulo, C. P.; Ford, M. J.; Searles, K.; Majidi, C.; Ware, T. H. 4D-Printable Liquid Metal−Liquid Crystal Elastomer Composites. *ACS Appl. Mater. Interfaces.* **2021**, *13* (11), 12805−12813.
(102) Wang, Z.; Wang, Z.; Zheng, Y.; He, Q.; Wang, Y.; Cai, S. Three-dimensional printing of functionally graded liquid crystal elastomer. *Sci. Adv.* **2020**, *6* (39), No. eabc0034.
(103) Kotikian, A.; Morales, J. M.; Lu, A.; Mueller, J.; Davidson, Z. S.; Boley, J. W.; Lewis, J. A. Innervated, Self-Sensing Liquid Crystal Elastomer Actuators with Closed Loop Control. *Adv. Mater.* **2021**, *33* (27), No. 2101814.
(104) Saed, M. O.; Ambulo, C. P.; Kim, H.; De, R.; Raval, V.; Searles, K.; Siddiqui, D. A.; Cue, J. M. O.; Stefan, M. C.; Shankar, M. R.; Ware,

T. H. Molecularly-Engineered, 4D-Printed Liquid Crystal Elastomer Actuators. *Adv. Funct. Mater.* **2019**, *29* (3), No. 1806412.
(105) Zou, W.; Lin, X.; Terentjev, E. M. Amine-Acrylate Liquid Single Crystal Elastomers Reinforced by Hydrogen Bonding. *Adv. Mater.* **2021**, *33* (30), No. 2101955.
(106) Liao, W.; Yang, Z. 3D printing programmable liquid crystal elastomer soft pneumatic actuators. *Mater. Horiz.* **2023**, *10* (2), 576−584.
(107) Roach, D. J.; Yuan, C.; Kuang, X.; Li, V. C.-F.; Blake, P.; Romero, M. L.; Hammel, I.; Yu, K.; Qi, H. J. Long Liquid Crystal Elastomer Fibers with Large Reversible Actuation Strains for Smart Textiles and Artificial Muscles. *ACS Appl. Mater. Interfaces.* **2019**, *11* (21), 19514−19521.
(108) Peng, X.; Wu, S.; Sun, X.; Yue, L.; Montgomery, S. M.; Demoly, F.; Zhou, K.; Zhao, R. R.; Qi, H. J. 4D Printing of Freestanding Liquid Crystal Elastomers via Hybrid Additive Manufacturing. *Adv. Mater.* **2022**, *34* (39), No. 2204890.
(109) Wang, Y.; Guan, Q.; Lei, D.; Esmaeely Neisiany, R.; Guo, Y.; Gu, S.; You, Z. Meniscus-Climbing System Inspired 3D Printed Fully Soft Robotics with Highly Flexible Three-Dimensional Locomotion at the Liquid−Air Interface. *ACS Nano* **2022**, *16* (11), 19393−19402.
(110) Wang, Y.; Yin, R.; Jin, L.; Liu, M.; Gao, Y.; Raney, J.; Yang, S. 3D-Printed Photoresponsive Liquid Crystal Elastomer Composites for Free-Form Actuation. *Adv. Funct. Mater.* **2023**, *33* (4), No. 2210614.
(111) Chen, M.; Hou, Y.; An, R.; Qi, H. J.; Zhou, K. 4D Printing of Reprogrammable Liquid Crystal Elastomers with Synergistic Photochromism and Photoactuation. *Adv. Mater.* **2023**, No. 2303969.
(112) Wang, Q.; Tian, X.; Zhang, D.; Zhou, Y.; Yan, W.; Li, D. Programmable spatial deformation by controllable off-center free-standing 4D printing of continuous fiber reinforced liquid crystal elastomer composites. *Nat. Commun.* **2023**, *14* (1), 3869.
(113) Lugger, S. J. D.; Verbroekken, R. M. C.; Mulder, D. J.; Schenning, A. P. H. J. Direct Ink Writing of Recyclable Supramolecular Soft Actuators. *ACS Macro Lett.* **2022**, *11* (7), 935−940.
(114) McDougall, L.; Herman, J.; Huntley, E.; Leguizamon, S.; Cook, A.; White, T.; Kaehr, B.; Roach, D. J. Free-Form Liquid Crystal Elastomers via Embedded 4D Printing. *ACS Appl. Mater. Interfaces.* **2023**, *15* (50), 58897−58904.
(115) Zeng, H.; Martella, D.; Wasylczyk, P.; Cerretti, G.; Lavocat, J.-C. G.; Ho, C.-H.; Parmeggiani, C.; Wiersma, D. S. High-Resolution 3D Direct Laser Writing for Liquid-Crystalline Elastomer Microstructures. *Adv. Mater.* **2014**, *26* (15), 2319−2322.
(116) Guo, Y.; Zhang, J.; Hu, W.; Khan, M. T. A.; Sitti, M. Shape-programmable liquid crystal elastomer structures with arbitrary three-dimensional director fields and geometries. *Nat. Commun.* **2021**, *12* (1), 5936.
(117) Chen, L.; Dong, Y.; Tang, C.-Y.; Zhong, L.; Law, W.-C.; Tsui, G. C. P.; Yang, Y.; Xie, X. Development of Direct-Laser-Printable Light-Powered Nanocomposites. *ACS Appl. Mater. Interfaces.* **2019**, *11* (21), 19541−19553.
(118) Yeung, K.-W.; Dong, Y.; Chen, L.; Tang, C.-Y.; Law, W.-C.; Tsui, G. C.-P.; Engstrom, D. S. Printability of photo-sensitive nanocomposites using two-photon polymerization. *Nanotechnol. Rev.* **2020**, *9* (1), 418−426.
(119) Tabrizi, M.; Ware, T. H.; Shankar, M. R. Voxelated Molecular Patterning in Three-Dimensional Freeforms. *ACS Appl. Mater. Interfaces.* **2019**, *11* (31), 28236−28245.
(120) Li, S.; Bai, H.; Liu, Z.; Zhang, X.; Huang, C.; Wiesner, L. W.; Silberstein, M.; Shepherd, R. F. Digital light processing of liquid crystal elastomers for self-sensing artificial muscles. *Sci. Adv.* **2021**, *7* (30), No. eabg3677.
(121) Fang, M.; Liu, T.; Xu, Y.; Jin, B.; Zheng, N.; Zhang, Y.; Zhao, Q.; Jia, Z.; Xie, T. Ultrafast Digital Fabrication of Designable Architectured Liquid Crystalline Elastomer. *Adv. Mater.* **2021**, *33* (52), No. 2105597.
(122) Jin, B.; Liu, J.; Shi, Y.; Chen, G.; Zhao, Q.; Yang, S. Solvent-Assisted 4D Programming and Reprogramming of Liquid Crystalline Organogels. *Adv. Mater.* **2022**, *34* (5), No. 2107855.
(123) Chen, G.; Jin, B.; Shi, Y.; Zhao, Q.; Shen, Y.; Xie, T. Rapidly and Repeatedly Reprogrammable Liquid Crystalline Elastomer via a Shape Memory Mechanism. *Adv. Mater.* **2022**, *34* (21), No. 2201679.
(124) Javadzadeh, M.; del Barrio, J.; Sánchez-Somolinos, C. Melt Electrowriting of Liquid Crystal Elastomer Scaffolds with Programmed Mechanical Response. *Adv. Mater.* **2023**, *35* (14), No. 2209244.
(125) Feng, X.; Wang, L.; Xue, Z.; Xie, C.; Han, J.; Pei, Y.; Zhang, Z.; Guo, W.; Lu, B. Melt electrowriting enabled 3D liquid crystal elastomer structures for cross-scale actuators and temperature field sensors. *Sci. Adv.* **2024**, *10* (10), No. eadk3854.
(126) Zhai, F.; Feng, Y.; Li, Z.; Xie, Y.; Ge, J.; Wang, H.; Qiu, W.; Feng, W. 4D-printed untethered self-propelling soft robot with tactile perception: Rolling, racing, and exploring. *Matter.* **2021**, *4* (10), 3313−3326.
(127) Montesino, L.; Martínez, J. I.; Sánchez-Somolinos, C. Reprogrammable 4D Printed Liquid Crystal Elastomer Photoactuators by Means of Light-Reversible Perylene Diimide Radicals. *Adv. Funct. Mater.* **2023**, No. 2309019.
(128) Vinciguerra, M. R.; Patel, D. K.; Zu, W.; Tavakoli, M.; Majidi, C.; Yao, L. Multimaterial Printing of Liquid Crystal Elastomers with Integrated Stretchable Electronics. *ACS Appl. Mater. Interfaces.* **2023**, *15* (20), 24777−24787.
(129) Choi, J.; Choi, Y.; Lee, J.-H.; Kim, M. C.; Park, S.; Hyun, K.; Lee, K. M.; Yoon, T.-H.; Ahn, S.-k. Direct-Ink-Written Cholesteric Liquid Crystal Elastomer with Programmable Mechanochromic Response. *Adv. Funct. Mater.* **2023**, No. 2310658.
(130) Yang, X.; Valenzuela, C.; Zhang, X.; Chen, Y.; Yang, Y.; Wang, L.; Feng, W. Robust integration of polymerizable perovskite quantum dots with responsive polymers enables 4D-printed self-deployable information display. *Matter.* **2023**, *6* (4), 1278−1294.
(131) Sol, J. A. H. P.; Smits, L. G.; Schenning, A. P. H. J.; Debije, M. G. Direct Ink Writing of 4D Structural Colors. *Adv. Funct. Mater.* **2022**, *32* (30), No. 2201766.
(132) Geng, Y.; Kizhakidathazhath, R.; Lagerwall, J. P. F. Robust cholesteric liquid crystal elastomer fibres for mechanochromic textiles. *Nat. Mater.* **2022**, *21* (12), 1441−1447.
(133) Bi, R.; Li, X.; Ou, X.; Huang, J.; Huang, D.; Chen, G.; Sheng, Y.; Hong, W.; Wang, Y.; Hu, W.; Guo, S.-Z. 3D-Printed Biomimetic Structural Colors. *Small.* **2024**, *20*, No. 2306646.
(134) Mistry, D.; Traugutt, N. A.; Sanborn, B.; Volpe, R. H.; Chatham, L. S.; Zhou, R.; Song, B.; Yu, K.; Long, K. N.; Yakacki, C. M. Soft elasticity optimises dissipation in 3D-printed liquid crystal elastomers. *Nat. Commun.* **2021**, *12* (1), 6677.
(135) Maurin, V.; Chang, Y.; Ze, Q.; Leanza, S.; Wang, J.; Zhao, R. R. Liquid Crystal Elastomer−Liquid Metal Composite: Ultrafast, Untethered, and Programmable Actuation by Induction Heating. *Adv. Mater.* **2023**, No. 2302765.
(136) Roach, D. J.; Sun, X.; Peng, X.; Demoly, F.; Zhou, K.; Qi, H. J. 4D Printed Multifunctional Composites with Cooling-Rate Mediated Tunable Shape Morphing. *Adv. Funct. Mater.* **2022**, *32* (36), No. 2203236.
(137) Sol, J. A. H. P.; Sentjens, H.; Yang, L.; Grossiord, N.; Schenning, A. P. H. J.; Debije, M. G. Anisotropic Iridescence and Polarization Patterns in a Direct Ink Written Chiral Photonic Polymer. *Adv. Mater.* **2021**, *33* (39), No. 2103309.
(138) Sol, J. A. H. P.; Douma, R. F.; Schenning, A. P. H. J.; Debije, M. G. 4D Printed Light-Responsive Patterned Liquid Crystal Elastomer Actuators Using a Single Structural Color Ink. *Adv. Mater. Technol.* **2023**, *8* (3), No. 2200970.
(139) Sun, Y.; Wang, L.; Zhu, Z.; Li, X.; Sun, H.; Zhao, Y.; Peng, C.; Liu, J.; Zhang, S.; Li, M. A 3D-Printed Ferromagnetic Liquid Crystal Elastomer with Programmed Dual-Anisotropy and Multi-Responsiveness. *Adv. Mater.* **2023**, *35* (45), No. 2302824.
(140) Zeng, H.; Wasylczyk, P.; Cerretti, G.; Martella, D.; Parmeggiani, C.; Wiersma, D. S. Alignment engineering in liquid crystalline elastomers: Free-form microstructures with multiple functionalities. *Appl. Phys. Lett.* **2015**, *106* (11), No. 111902.

https://doi.org/10.1021/cbe.4c00027
Chem Bio Eng. 2024, 1, 488−515

(141) Mainik, P.; Hsu, L.-Y.; Zimmer, C. W.; Fauser, D.; Steeb, H.; Blasco, E. DLP 4D Printing of Multi-Responsive Bilayered Structures. *Adv. Mater. Technol.* **2023**, *8* (23), No. 2300727.
(142) Tian, X.; Guo, Y.; Zhang, J.; Ivasishin, O. M.; Jia, J.; Yan, J. Fiber Actuators Based on Reversible Thermal Responsive Liquid Crystal Elastomer. *Small.* **2024**, No. 2306952.
(143) Escobar, M. C.; White, T. J. Fast and Slow-Twitch Actuation via Twisted Liquid Crystal Elastomer Fibers. *Adv. Mater.* **2024**, No. 2401140.
(144) Rešetič, A. Shape programming of liquid crystal elastomers. *Commun. Chem.* **2024**, *7* (1), 56.
(145) Traugutt, N. A.; Mistry, D.; Luo, C.; Yu, K.; Ge, Q.; Yakacki, C. M. Liquid-Crystal-Elastomer-Based Dissipative Structures by Digital Light Processing 3D Printing. *Adv. Mater.* **2020**, *32* (28), No. 2000797.
(146) Kotikian, A.; Watkins, A. A.; Bordiga, G.; Spielberg, A.; Davidson, Z. S.; Bertoldi, K.; Lewis, J. A. Liquid Crystal Elastomer Lattices with Thermally Programmable Deformation via Multi-Material 3D Printing. *Adv. Mater.* **2024**, No. 2310743.
(147) Jin, B.; Chen, G.; Chen, Y.; Yang, C.; Zhu, Z.; Weng, Y.; Zhao, Q.; Xie, T. Reprogramming Photoresponsive Liquid Crystalline Elastomer via Force-Directed Evaporation. *ACS Appl. Mater. Interfaces.* **2024**, *16* (13), 16844−16852.
(148) Ilami, M.; Bagheri, H.; Ahmed, R.; Skowronek, E. O.; Marvi, H. Materials, Actuators, and Sensors for Soft Bioinspired Robots. *Adv. Mater.* **2021**, *33* (19), No. 2003139.
(149) Xiong, J.; Chen, J.; Lee, P. S. Functional Fibers and Fabrics for Soft Robotics, Wearables, and Human−Robot Interface. *Adv. Mater.* **2021**, *33* (19), No. 2002640.
(150) Li, M.; Pal, A.; Aghakhani, A.; Pena-Francesch, A.; Sitti, M. Soft actuators for real-world applications. *Nat. Rev. Mater.* **2022**, *7* (3), 235−249.
(151) Shih, B.; Shah, D.; Li, J.; Thuruthel, T. G.; Park, Y.-L.; Iida, F.; Bao, Z.; Kramer-Bottiglio, R.; Tolley, M. T. Electronic skins and machine learning for intelligent soft robots. *Sci. Robot.* **2020**, *5* (41), No. eaaz9239.
(152) Yang, Y.; Wu, Y.; Li, C.; Yang, X.; Chen, W. Flexible Actuators for Soft Robotics. *Adv. Intell. Syst.* **2020**, *2* (1), No. 1900077.
(153) Whitesides, G. M. Soft Robotics. *Angew. Chem. Int. Ed.* **2018**, *57* (16), 4258−4273.
(154) Pilz da Cunha, M.; Ambergen, S.; Debije, M. G.; Homburg, E. F. G. A.; den Toonder, J. M. J.; Schenning, A. P. H. J. A Soft Transporter Robot Fueled by Light. *Adv. Sci.* **2020**, *7* (5), No. 1902842.
(155) Hu, J.; Nie, Z.; Wang, M.; Liu, Z.; Huang, S.; Yang, H. Springtail-inspired Light-driven Soft Jumping Robots Based on Liquid Crystal Elastomers with Monolithic Three-leaf Panel Fold Structure. *Angew. Chem. Int. Ed.* **2023**, *62* (9), No. e202218227.
(156) Rogóż, M.; Zeng, H.; Xuan, C.; Wiersma, D. S.; Wasylczyk, P. Light-Driven Soft Robot Mimics Caterpillar Locomotion in Natural Scale. *Adv. Opt. Mater.* **2016**, *4* (11), 1689−1694.
(157) Ahn, C.; Liang, X.; Cai, S. Bioinspired Design of Light-Powered Crawling, Squeezing, and Jumping Untethered Soft Robot. *Adv. Mater. Technol.* **2019**, *4* (7), No. 1900185.
(158) Pang, X.; Lv, J.-a.; Zhu, C.; Qin, L.; Yu, Y. Photodeformable Azobenzene-Containing Liquid Crystal Polymers and Soft Actuators. *Adv. Mater.* **2019**, *31* (52), No. 1904224.
(159) Yamada, M.; Kondo, M.; Mamiya, J.-i.; Yu, Y.; Kinoshita, M.; Barrett, C. J.; Ikeda, T. Photomobile Polymer Materials: Towards Light-Driven Plastic Motors. *Angew. Chem. Int. Ed.* **2008**, *47* (27), 4986−4988.
(160) Gao, R. Z.; Ren, C. L. Synergizing microfluidics with soft robotics: A perspective on miniaturization and future directions. *Biomicrofluidics* **2021**, *15* (1), No. 011302.
(161) Sun, D.; Zhang, J.; Li, H.; Shi, Z.; Meng, Q.; Liu, S.; Chen, J.; Liu, X. Toward Application of Liquid Crystalline Elastomer for Smart Robotics: State of the Art and Challenges. *Polymers* **2021**, *13* (11), 1889.
(162) Wang, Y.; Sun, J.; Liao, W.; Yang, Z. Liquid Crystal Elastomer Twist Fibers toward Rotating Microengines. *Adv. Mater.* **2022**, *34* (9), No. 2107840.
(163) McCracken, J. M.; Donovan, B. R.; White, T. J. Materials as Machines. *Adv. Mater.* **2020**, *32* (20), No. 1906564.
(164) Martinez, A. M.; McBride, M. K.; White, T. J.; Bowman, C. N. Reconfigurable and Spatially Programmable Chameleon Skin-Like Material Utilizing Light Responsive Covalent Adaptable Cholesteric Liquid Crystal Elastomers. *Adv. Funct. Mater.* **2020**, *30* (35), No. 2003150.
(165) Kim, S.-U.; Lee, Y.-J.; Liu, J.; Kim, D. S.; Wang, H.; Yang, S. Broadband and pixelated camouflage in inflating chiral nematic liquid crystalline elastomers. *Nat. Mater.* **2022**, *21* (1), 41−46.
(166) Rus, D.; Tolley, M. T. Design, fabrication and control of origami robots. *Nat. Rev. Mater.* **2018**, *3* (6), 101−112.
(167) Volpe, R. H.; Mistry, D.; Patel, V. V.; Patel, R. R.; Yakacki, C. M. Dynamically Crystalizing Liquid-Crystal Elastomers for an Expandable Endplate-Conforming Interbody Fusion Cage. *Adv. Healthc. Mater.* **2020**, *9* (1), No. 1901136.
(168) Merkel, D. R.; Shaha, R. K.; Yakacki, C. M.; Frick, C. P. Mechanical energy dissipation in polydomain nematic liquid crystal elastomers in response to oscillating loading. *Polymer* **2019**, *166*, 148−154.
(169) Ohzono, T.; Katoh, K.; Minamikawa, H.; Saed, M. O.; Terentjev, E. M. Internal constraints and arrested relaxation in main-chain nematic elastomers. *Nat. Commun.* **2021**, *12* (1), 787.
(170) Huang, C.; Chen, L. Negative Poisson's Ratio in Modern Functional Materials. *Adv. Mater.* **2016**, *28* (37), 8079−8096.
(171) Luo, C.; Chung, C.; Traugutt, N. A.; Yakacki, C. M.; Long, K. N.; Yu, K. 3D Printing of Liquid Crystal Elastomer Foams for Enhanced Energy Dissipation Under Mechanical Insult. *ACS Appl. Mater. Interfaces.* **2021**, *13* (11), 12698−12708.
(172) Larson, N. M.; Mueller, J.; Chortos, A.; Davidson, Z. S.; Clarke, D. R.; Lewis, J. A. Rotational multimaterial printing of filaments with subvoxel control. *Nature.* **2023**, *613* (7945), 682−688.
(173) Wang, Z.; Cai, S. Recent progress in dynamic covalent chemistries for liquid crystal elastomers. *J. Mater. Chem. B* **2020**, *8* (31), 6610−6623.
(174) Ube, T.; Suka, I.; Ogikubo, S.; Hashimoto, G.; Suda, M.; Yamamoto, H. M.; Ikeda, T. Inducing Motions of Polymers in Liquid Nitrogen with Light. *Adv. Mater.* **2023**, *35* (47), No. 2306402.
(175) Wang, Y.; Xuan, H.; Zhang, L.; Huang, H.; Neisiany, R. E.; Zhang, H.; Gu, S.; Guan, Q.; You, Z. 4D Printed Non-Euclidean-Plate Jellyfish Inspired Soft Robot in Diverse Organic Solvents. *Adv. Mater.* **2024**, *36* (16), No. 2313761.

https://doi.org/10.1021/cbe.4c00027
Chem Bio Eng. 2024, 1, 488−515